CHARLES UNIVERSITY

Faculty of Pharmacy in Hradec Králové

Department of Organic and Bioorganic Chemistry

Synthesis of fluorinated serine derivatives and study of their effect on skin barrier function

Diploma thesis

Richard Župina

Hradec Králové 2022

Supervisor: Prof. PharmDr. Kateřina Vávrová, Ph.D.

Consultant: Dr. Georgios Paraskevopoulos, Ph.D.

Prohlašuji, že tato práce je mým původním autorským dílem, které jsem vypracoval samostatně (pod vedením konzultanta). Veškerá literatura a další zdroje, z nichž jsem při zpracování čerpal, jsou uvedeny v seznamu použité literatury a v práci řádně citovány. Práce nebyla využita k získání jiného nebo stejného titulu.

V Hradci Králové 2022 Richard Župina

Acknowledgments

In this way I would like to thank the supervisor of this diploma thesis Prof. PharmDr. Kateřina Vávrová Ph.D. and consultant Dr. Georgios Paraskevopoulos Ph.D. for their time, valuable advice and overall guidance during my work in the lab and writing this thesis. Next, I would like to thank all members of the Skin Barrier Research Group for their time and cooperation. I would also like to thank all members of the Department of Organic and Bioorganic Chemistry and the Department of Pharmaceutical Technology. Finally, a special gratitude to my family and friends for their mental support.

For the financial support I would like to thank Charles University (SVV 260 547) and Grant Agency of Czech Republic (GAČR 19-09600S).

Abstrakt

Univerzita Karlova, Farmaceutická fakulta v Hradci Králové

Katedra Organické a Bioorganické Chemie

Školitel: Prof. PharmDr. Kateřina Vávrová, Ph.D.

Konzultant: Dr. Georgios Paraskevopoulos, Ph.D.

Autor: Richard Župina

Název diplomové práce: Syntéza fluorovaných derivátov serínu a štúdium ich vplyvu na bariérovú funkciu kože

Ľudská koža slúži ako bariéra proti fyzickému, chemickému a mikrobiálnemu poškodeniu. Ak je kožná bariéra narušená, dochádza k možnosti infiltrácie mikróbov a biochemického poškodenia. Ceramidy slúžia ako základné zložky lipidovej vrstvy pokožky, čím napomáhajú udržiavať integritu kožnej bariéry. Znížený obsah epidermálnych ceramidov súvisí s kožnými ochoreniami, ako je atopická dermatitída a psoriáza. Predchádzajúce zistenia našej výskumnej skupiny preukázali, že molekula analogická k ceramidom nachádzajúcim sa v epiderme, ktorá má podobné sterické a hydrofóbne vlastnosti, by mohla suplementovať nedostatok ceramidov v *stratum corneum* jednoduchým fyzikálno-chemickým pôsobením.

Cieľom tejto štúdie bolo navrhnúť jednoduchú syntézu molekúl analogických ku kožným ceramidom vychádzajúcich zo štruktúry L-serínu s dvoma dlhými alifatickými reťazcami. Prvý reťazec pochádza z kyseliny lignocerovej viazanej amidovou väzbou k zbytku molekuly a druhý reťazec je buď 10 alebo 14 uhlíkový polyfluorovaný reťazec spojený so zbytkom molekuly cez esterovú väzbu. Ďalej bolo cieľom otestovať potenciálnu schopnosť syntetizovaných zlúčenín kontrolovane obnovovať poškodenú ľudskú kožnú bariéru a porovnať túto schopnosť s ich nefluórovými analogickými zlúčeninami.

Permeačné experimenty s novo syntetizovanými polyfluorovanými molekulami analogickými k ceramidom v ľudskej koži ukázali mierne zlepšenie kožných bariérových vlastností u predtým poškodeného stratum corneum. Avšak obe polyfluorované molekuly mali horšie výsledky v porovnaní s ich nefluórovými analogickými zlúčeninami, s tým že molekula s 10 uhlíkovým fluorovaným reťazcom mala oveľa lepší permeačný profil ako molekula so 14 uhlíkovým fluorovaným reťazcom.

Na prvý pohľad je možné z výsledkov vyčítať že polyfluorácia molekúl nevylepšila ich schopnosť obnovovať poškodenú kožu. Je ale dôležité spomenúť problémy

s rozpustnosťou týchto molekúl v bežných rozpúšťadlách. Znížená rozpustnosť vo vehikule by mohla viesť k nedostatočnému vplyvu zlúčenín na poškodené *stratum corneum*. Preto je nasledujúcim cieľom nájsť iné možnosti aplikačných podmienok, aby bolo možné sledovať vplyv fluorácie spoľahlivejšie.

Abstract

Charles University, Faculty of Pharmacy in Hradec Králové

Department of Organic and Bioorganic Chemistry

Supervisor: Prof. PharmDr. Kateřina Vávrová, Ph.D.

Consultant: Dr. Georgios Paraskevopoulos, Ph.D.

Author: Richard Župina

Title of the thesis: Synthesis of fluorinated serine derivatives and study of their effect on skin barrier function

The human skin serves as a barrier against physical, chemical and microbial injury. When the skin barrier is perturbed, there is a possibility of microbial infiltration and biochemical damage. Ceramides, as essential components of the skin lipid layer, help to maintain the barrier integrity. Decreased content of skin ceramides in epidermis is connected with skin diseases such as atopic dermatitis and psoriasis. Previous findings of our research group proved that a ceramide analogue with similar steric and hydrophobic parameters to skin ceramides could selectively supplement the recovery of perturbed human skin barrier.

The goal of this study was to design a convenient synthesis of ceramide analogues derived from L-serine with two long aliphatic chains. The first chain is amidically bound lignoceric acid and the second chain is either a 10 or a 14 carbon polyfluorinated chain conjugated with the rest of the molecule by an ester bond. Furthermore, the aim of this study was to test the potential ability of synthesized compounds to recover a controllably perturbed human skin barrier in comparison with their non-fluorinated analogues.

Permeation experiments with the newly synthesized polyfluorinated ceramide analogues have shown a slight improvement in skin barrier properties of previously damaged human stratum corneum. However, both 10 and 14 carbon fluorinated derivatives have shown worse results than their non-fluorinated analogues, with the former having much better permeation profile than the latter.

From the results, the first idea is that polyfluorination did not improve the skin repairing ability of the molecules. However, it is vital to mention the struggles with low solubility of polyfluorinated compounds in common solvents. This could lead to insufficient impact on the damaged stratum corneum. Therefore, the future approach is to find an alternative application conditions for these compounds in order to observe the influence of the polyfluorination more reliably.

Table of Contents

1. List of abbreviations

AD	Atopic Dermatitis
Bn	Benzyl
Boc	*tert*-butyloxycarbonyl
Cer	Ceramide
CerS	Ceramide synthase
CoA	Coenzyme A
DCM	Dichloromethane
DMAP	4-Dimethylaminopyridine
EDC	1-Ethyl-3-(3-dimethylaminopropyl)-carbodiimide
EI	Electrical impedance
ELOVL	Elongation of very long chain fatty acids protein
Eq	Equivalent
FA2H	Fatty acid 2-hydroxylase
HPLC	High performance liquid chromatography
IL-8	Interleukin 8
IR	Infrared spectroscopy
Mp	Melting point
MS	Mass spectrometry
NMR	Nuclear magnetic resonance
PBS	Phosphate-buffered saline
pCer	Pseudoceramide
PG	Propylene glycol
R_f	Retention factor

SC	Stratum corneum
SCORAD	Scoring atopic dermatitis
SPT	Serine palmitoyl transferase
TEWL	Transepidermal water loss
TLC	Thin layer chromatography
TNF-α	Tumor necrosis factor alpha

2. Introduction and Aim of the work

Human skin, amongst many other functions, carries out protecting function for the entire body. *Stratum corneum (SC),* as the outermost layer of epidermis and the whole skin, is the most significant barrier maintaining layer. It is composed of corneocytes with robust - almost impermeable - membrane and a mixture of lipids (ceramides (Cer), free fatty acids and cholesterol). Cer are molecules with unique hydro/lipophilic properties, which allow them to maintain the protective function of the skin. Many diseases have been connected with skin Cer content decrease and alteration. Amongst those are for example atopic dermatitis (AD), psoriasis and many more. Improvement of symptoms in these diseases after Cer substitutional therapy (Cer rich emollients) has been described. Although Cer are very complex molecules, there is a continuous pursuit to find a more convenient way for their synthesis or to develop molecules that are structurally similar and can mimic their properties (pseudoceramides (pCer)). Many molecules have been synthesized, used as Cer analogues and shown comparable effects. Some of them exhibited skin permeation enhancing ability. However, after extensive fluorination this ability was abolished.

The first aim of this work was to conveniently synthesize Cer analogues, L-serine derivatives that have lignoceric acid bound to the primary amine *via* an amide bond and 10 and 14 polyfluorinated carbon chain attached by an ester bond. (Figure 1). The second aim was to find a controllable way of damaging the SC, treat this SC with the polyfluorinated compounds, using healthy SC as a control, and carry out a permeation experiment using theophylline as a model permeant. The aim of the skin experiment was to investigate potential ability of the polyfluorinated derivatives to recover perturbed human SC more effectively than their non-fluorinated analogues.

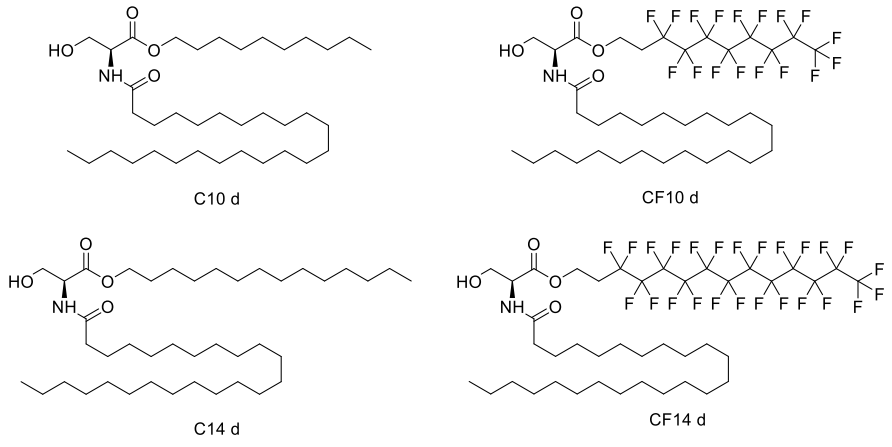

Figure 1 Summary of synthesized final compounds

3. Theoretical part

3.1. Human skin

Human skin is the largest organ covering the whole surface of the body and making up around 15% of the weight of a human adult.(1, 2) In fact, it is twice the weight of brain, around 3 to 5 kg.(3) Its thickness varies from 0.5 mm to 4 mm depending on the body's part.(2) Human skin serves as a primary biochemical and mechanical barrier. It regulates body temperature and water loss, by which the body retains homeostasis. It serves endocrine function, by production of vitamin D, but also exocrine function, *via* sebaceous and sweat glands. Skin also plays an important role as a sense organ *via* nervous tissue called nociceptors.(1, 4)

Skin is composed of three main layers. The outermost layer is called epidermis, the middle layer is called dermis and the innermost layer is called hypodermis (Figure 2).

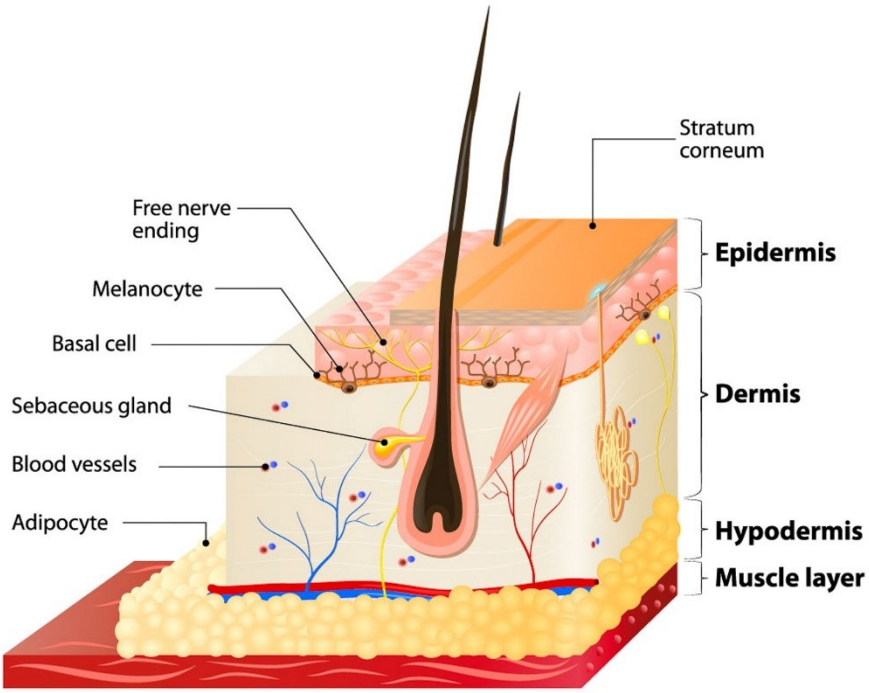

Figure 2 Layers of skin

Source https://naoscare.ae/blogs/hazar-elkhoury-blog/the-structure-of-skin

The deepest part of the skin, hypodermis, consists mainly of adipocytes in a form of lobules separated by connective tissue. It divides muscular tissue from dermis and epidermis and serves for thermoregulation, protection, insulation, and source of energy.(1, 5)

Skin's middle part - dermis, also known as corium - can be divided into two sublayers. The deeper and denser sublayer, *stratum reticulare*, is responsible for mechanical

rigidity. It consists of densely bundled collagen fibrils at the expense of elastic fibrils. *Stratum papillare*, the outer sublayer of the dermis, consists of several types of cells (fibroblasts, dendrocytes, mast cells) and has abundant vascularization and innervation. This sublayer forms conical, perpendicular structures that alternate with epidermal ridges leading to larger connection area and thus better adhesion between those two layers.(1, 2, 5)

Epidermis is the outermost layer of the skin. It is a continuously renewing striated squamous epithelial tissue made up mostly of keratin cells (95%). The rest (approx. 5%) consists of Langerhans cells, responsible for immune reaction, melanocytes, producing skin pigment melanin and Merkel cells functioning as mechanoreceptors.(1) The epidermis lacks vascularization and is dependent on dermis for metabolite exchange.(6) It can be divided into 5 sublayers:

- *Stratum basale* – It is the deepest sublayer of epidermis formed by a single line of keratinocytes capable of mitosis. One cell of every mitotic cycle ascends to following layers and the other one stays in *stratum basale.* Even though epidermis does not have any vascularization, this layer, as the closest one to the dermis, is nourished enough to undergo mitosis.(6) *Stratum basale* then contains melanocytes (one for every six cells)(3) and Merkel cells (smaller population than keratinocytes).(6)
- *Stratum spinosum* – Being from five to twelve cells thick, *stratum spinosum* consists of daughter cells of keratinocytes, that migrated from the previous layer. In this layer cells become rounder and join *via* desmosomes (intracellular bridges) (Figure 3), which are constantly breaking and renewing while the cells are moving towards higher layers.(6) Langerhans cells (Figure 3) can also be found in this layer.(3) They play a key role in recognizing potentially harmful microorganisms and are capable of destroying them.(6)
- *Stratum granulosum* – This layer comprises three to five layers. Here the keratinocytes elongate, lose their nucleus and become filled with keratin. In other words, in this layer the cells completely lose, their metabolic activity.(6) Keratohyalin granules (Figure 3) can also be found here. Keratohyalin is a protein structure, which is involved in keratinization, by converting keratin tonofilaments to homogenous matrix and thus transforming keratinocytes to corneocytes.(7) Another structure, that can be found here is an Odland's body, which is capable of producing precursors of barrier lipids.(6)
- *Stratum lucidum* – Made mostly of keratin filled dead cells with thickened plasma membrane, *stratum lucidum* can be found only in areas where the skin is thicker. These are fingertips, palms of hands and soles of feet, which also represent body parts with

no hair follicles. It is three to five layers of cells thick and provides a waterproofing effect to some extent.(6)

- *Stratum corneum* (SC) – This is the outermost layer of epidermis. Due to its importance for this work, this layer will be discussed more thoroughly in the next chapter

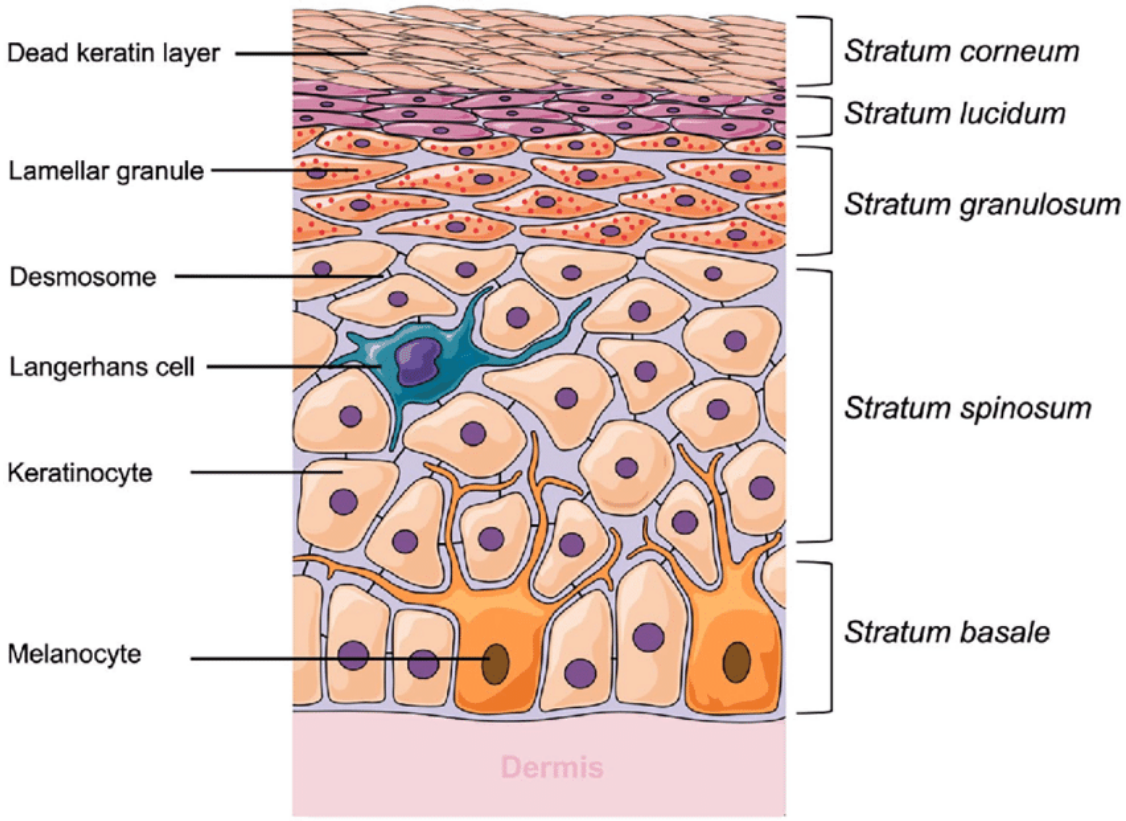

Figure 3 Layers of epidermis(8)

It takes roughly thirty days, for keratinocytes, to migrate from *stratum basale* to *stratum corneum* where they shed as corneocytes. Over this time, they become mature and subsequently undergo apoptosis and die. During this process they become more and more keratinized, therefore provide a mechanical protection from heat, chemicals and microorganisms. If the skin is healthy, there is a balance between mitosis and shedding of the corneocytes.(6)

3.2. Stratum corneum

SC, as the outermost layer of epidermis, plays a key role in protective function of the skin.(9) Prevention of excessive transepidermal water loss (TEWL) is another important function of this layer.(10) Structurally, SC comprises intercellularly connected corneocytes by corneodesmosomes. The corneocytes are further enriched with multilamellar lipid matrix to keep the layer intact and preserve its' hydrophobic properties. With this appearance it is often referred to as a brick wall-like structure (Figure 4).(11) There are approximately fifteen layers of these multi-organized cells being from 10 to 20 μm thick overall.(9) Corneocytes are mostly made up of a protein (keratin) and chemical composition of the SC is approximately 75% to 80% of this protein. Up to 15% of SC weight is water. Extracellular lipid matrix then makes up around 10% to 15% of its dry weight. When discussing the prevention of water loss and protective properties, lipids play a key role despite their small percentage. This is because the major pathway of molecule permeation is right through the lipids, since the corneocytes are too rigid to penetrate. Studies have shown that removal of only lipid matrix from epidermis led to same TEWL in comparison to removal of the whole SC layer.(12) Lipid matrix consists of diverse group of Cer, cholesterol and free fatty acids with content of 40 to 50%, 20 to 33% and 7 to 13% respectively.(9)

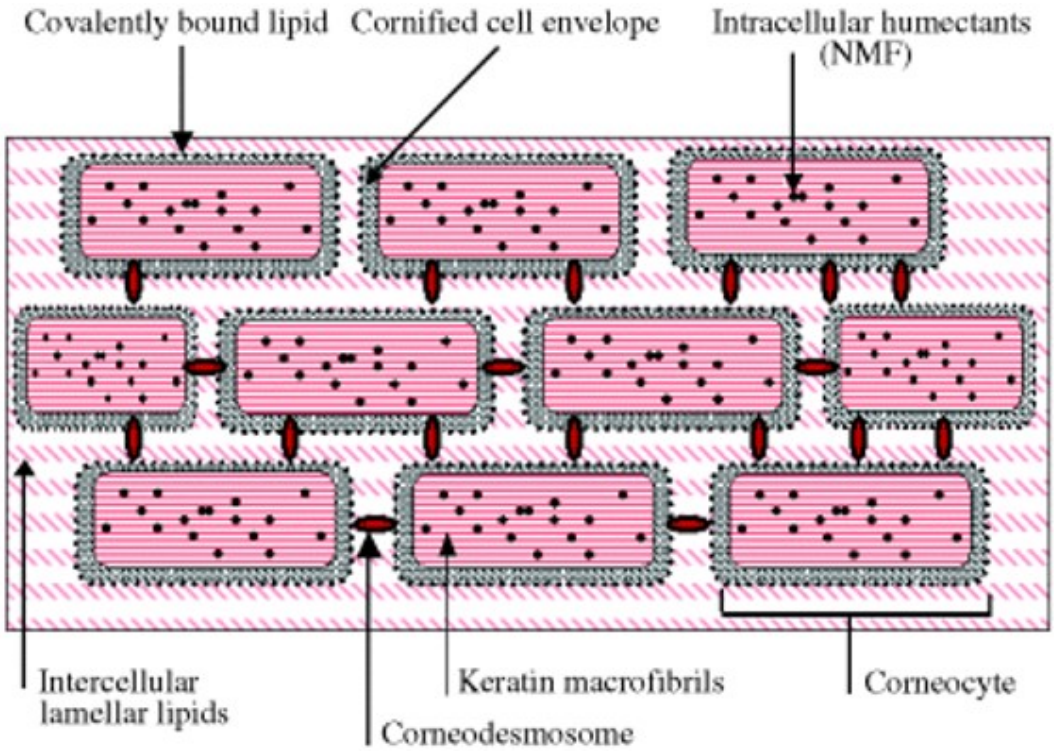

Figure 4 Brick wall model of SC

Source https://dermavidualsny.com/wp-content/uploads/2020/06/Brick-Mortar-Graphic.png

3.3. Ceramides

Cer are an essential part of the extracellular lipid matrix, which surrounds the corneocytes. They are the key components for maintenance of SC homeostasis.(13, 14) Dysregulation in Cer production can have various negative outcomes.(15) Skin Cer's backbone is a sphingoid base that is bound with a fatty acid of various length and structure *via* an amide bond.(16) With 4 major different types of Sphingoid bases and 3 major types of fatty acids found in skin (Figure 5), this makes up to 12 most common distinctive classes of ceramides. What makes the group even more diverse is that within these 12 classes, either base or acid can vary in length of the chain, which makes this group immensely diverse. (17) It is notable that there has been found up to 1000 species of Cer in human epidermis, most of them in SC. (18)

Sphingoid bases are basic amino alcohols with a long aliphatic chain. The aliphatic chain consists mostly of 12 to 22 carbon atoms.(19) The four major types of Sphingoid bases which can be found in SC are Sphingosine [S], Phytosphingosine [P], Dihydrosphingosine [dS] and 6-hydroxy Sphingosine [H] (Figure 5). A fatty acid, which is a long hydrophobic carbon chain with a polar head, is bound to a primary amine of the sphingoid base in a formation of amide bond. This fatty acid can be non-hydroxylated [N], α-hydroxylated [A] or ω-hydroxylated [EO] (Figure 5).(16, 20) ω-Hydroxy group of the latter is further esterified, and is usually a linoleate moiety.(20) Acid sidechain length varies from 14 to 30 - 40 carbon atoms. However predominantly chains of 20 and more carbon atoms could be found in SC.(16, 20)

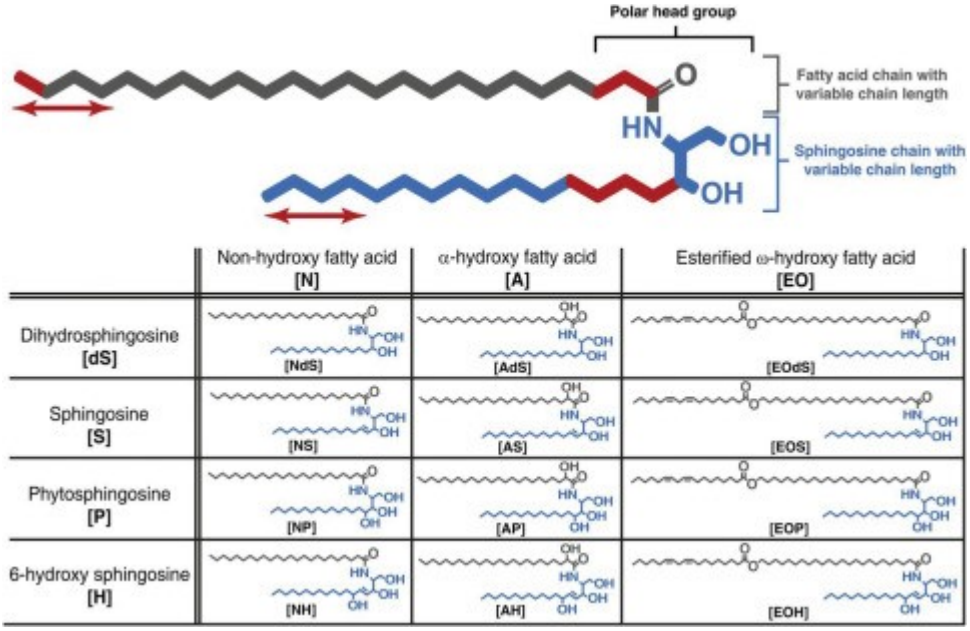

Figure 5 Classes of ceramides found in skin and their abbreviations.(22)

Cer consist of a polar head that contains several functional groups allowing the formation of lateral hydrogen bonds with the neighboring Cer. The polar head is relatively small in comparison to phospholipids. This allows more compact arrangement, and thus maintains rigidness of the SC.(23) However this fact alone would not be sufficient to guarantee the impermeability of water and other molecules. Fatty acids, both free and bound to sphingoid base, complement these properties. The fatty acids have long, usually saturated aliphatic chains with a small polar head group (carboxylic group). They have a high melting point and at physiological temperature retain a solid crystalline or a gel state. In these conditions they form an orthorhombic lateral packing and a membrane like this has lower lateral diffusion rates; thus, the molecules' permeability is much lower.(20, 23) This extraordinary lamellar arrangement could not be found in any other body organelle.(21)

3.4. Biosynthesis of Ceramides

Cer biosynthesis in mammalian skin cells is a complex, yet not completely understood process. One way of endogenous Cer synthesis is *de-novo* biosynthesis. The other way is a salvage pathway.

3.4.1. *De-novo* synthesis

De-novo Cer biosynthesis begins at endoplasmic reticulum. The first reaction is condensation of L-serine and acyl coenzyme A (CoA). This step is catalyzed by an enzyme called serine palmitoyl transferase (SPT). SPT is mediated by pyridoxal 5'-phosphate as a cofactor and this step serves as a rate-limiting step in Cer biosynthesis. L-Serine is typically condensed with a palmitoyl-CoA to form 18 carbon sphingoid base (3-ketodihydrosphingosine), as it is the most abundant in human skin.(24) However, the length of sphingoid base acyl chains can differ depending on SPT individual isoenzyme combination.(25) 3-Ketodihydrosphingosine is then reduced by 3-ketodihydrosphingosine reductase to form dihydrosphingosine. Dihydrosphingosine is subsequently *N*-acylated by Ceramide synthase (CerS) to form dihydroceramide. Dihydroceramide then undergoes either desaturation (catalyzed by dihydro-Cer desaturase) to form a Cer, or hydroxylation (catalyzed by dihydro-Cer hydroxylase) to form a phyto-Cer.(16, 26) Enzyme responsible for 6-hydroxy-Cer formation has not yet been identified (Figure 6).(27)

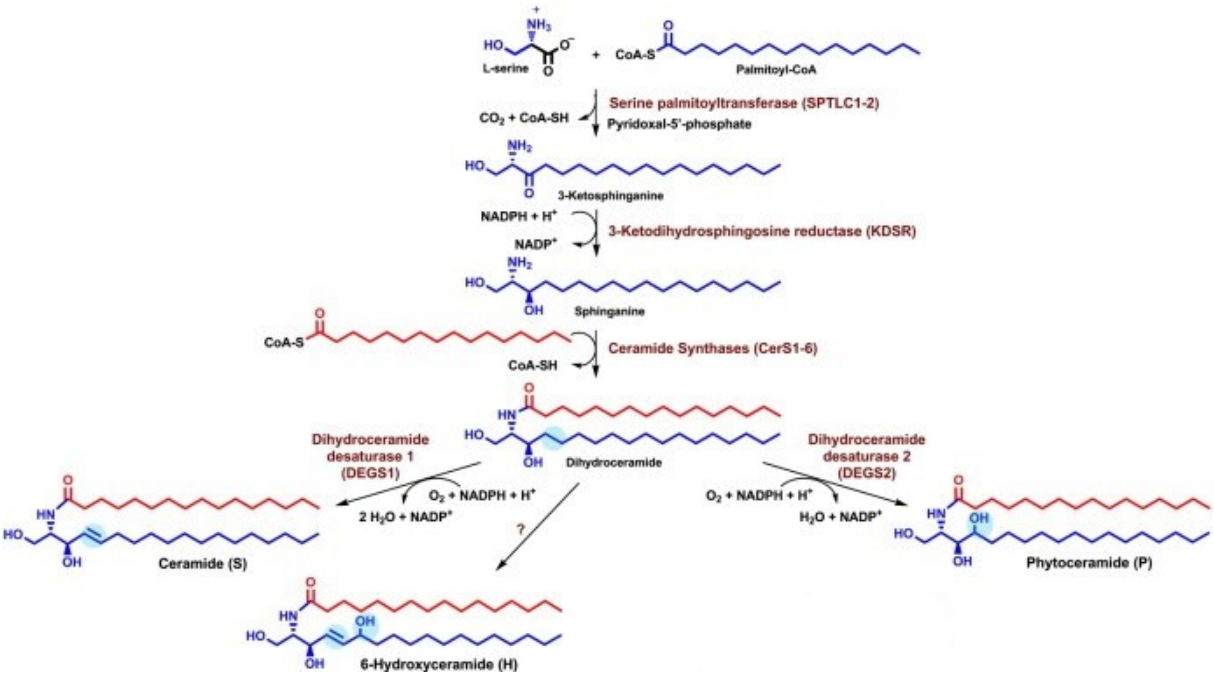

Figure 6 De-novo synthesis of Cer, 6-hydroxy-Cer, phyto-Cer (24)

CerS is an enzyme that has the ability to *N*-acylate various sphingoid bases and is responsible for immense diversity of Cer. CerS is also responsible for the attachment of free fatty acid chain to one of the sphingoid bases. There has been 6 distinct CerS identified in human body. Even though CerS have a broad spectrum of specificity, each of them has a particular acyl chain length preference.(26) Different studies have shown a various representation of CerS in different body tissues. In table 1, there is an overview of fatty acid preference and tissue expression of particular CerS. (27, 28) Fatty acids in bold show a strong preference of CerS. Tissues listed in brackets are the ones, where a particular CerS is most abundant. Upregulation of CerS 3 and 4 has been observed in suprabasal layers of epidermis where differentiated keratinocytes occur. These CerS, especially CerS 3, prefer much broader spectrum as well as higher lengths of fatty acid.(16)

Table 1 Fatty acid preference and tissue expression of different CerS

Number of CerS	Fatty acid preference	Tissue expression
CerS 1	C16:0, **C18:0**	Brain
CerS 2	C20:0, **C22:0**, **C24:0**, C26:0	Ubiquitous (Liver, Kidneys)
CerS 3	C18:0, C20:0, C22:0, C24:0, C26:0	Epidermis, Testis
CerS 4	**C18:0**, **C20:0**, C22:0, C24:0	Sebaceous glands, Lungs
CerS 5	C14:0, **C16:0**, C18:0, C18:1	Ubiquitous (Testis, Lung, Adipose tissue)
CerS 6	C14:0, **C16:0**, C18:0	Ubiquitous (Kidney, Intestine)

3.4.2. Salvage pathway

Salvage pathway, as the other way of Cer biosynthesis, lies in using free sphingoid bases which have been released after sphingolipid degradation. This process occurs in acidic environment of endosomes and lysosomes.(29) Sphingolipids break down to common metabolic product, a Cer, which cannot pass the lysosome membrane.(30) However, after acid ceramidase hydrolysis, it breaks down to a free fatty acid and free long chain sphingoid base. These catabolic products are able to pass freely from lysosome(31) to enter the *de-novo* pathway and form a Cer again. *N*-acylation of the "recycled" sphingoid bases is mediated by CerS presumably at the surface of endoplasmic reticulum.(29)

3.4.3. Formation of Free fatty acids for Cer biosynthesis.

Free fatty acids are formed *de-novo* in cytosol by a protein complex called fatty acid synthase. This repetitive cycle comprises four steps (condensation, reduction, dehydration and another reduction) and the acyl chain is elongated by two carbons during each cycle. Acetyl-CoA and malonyl-CoA, as a two-carbon donor, are condensed by an enzyme called 3-ketoacyl-CoA synthase forming 3-ketoacyl-CoA. 3-ketoacyl-CoA then undergoes reduction by the enzyme 3-ketoacyl-CoA reductase, thus forming 3-hydroxyacyl-CoA. The third step is a dehydration catalyzed by 3-hydroxyacyl-CoA dehydratase. The fourth and final step is the reduction of *trans*-2-enoyl-CoA to an acyl-CoA, which enters the cycle again condensing with another molecule of malonyl-CoA. The first reaction, condensation, is the rate-limiting step. This elongation cycle is repeated until palmitic acid molecule is produced (C16:0-COOH).(24, 27, 32)

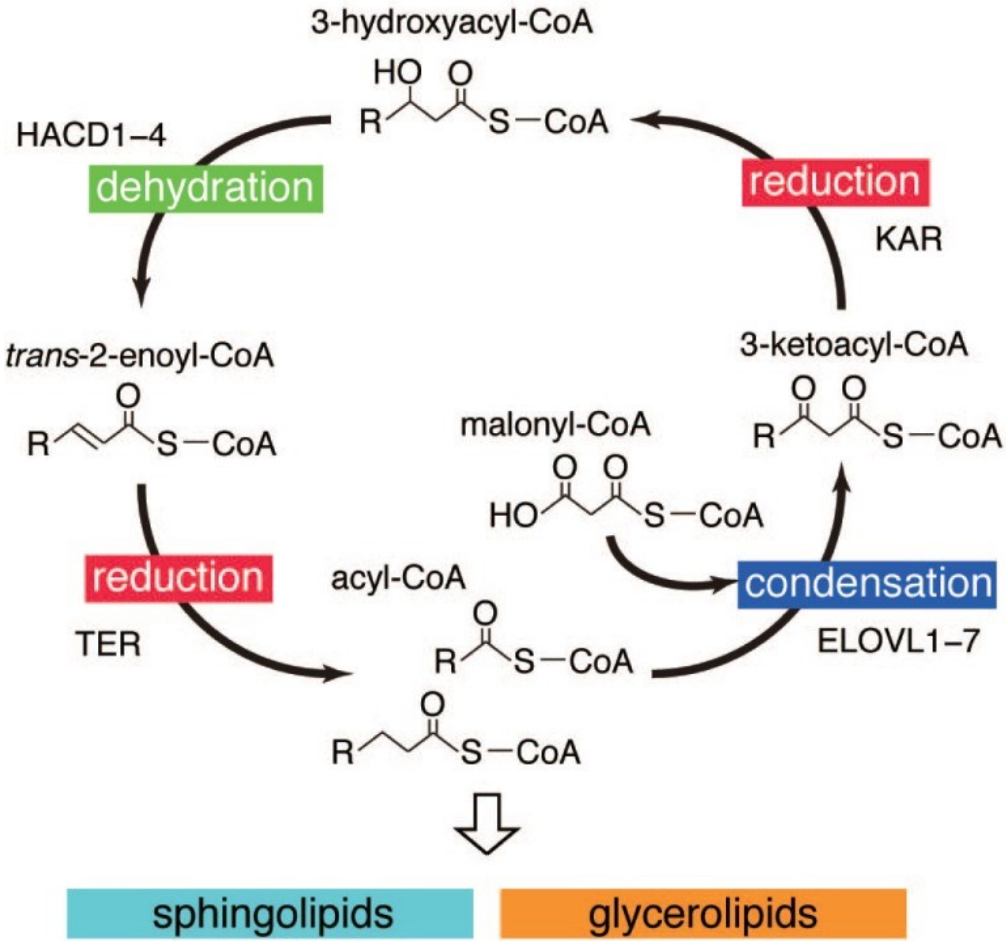

Figure 7 Elongation cycle of fatty acid synthesis(32)

Palmitic acid is then further elongated at endoplasmic reticulum to various lengths (Figure 7). This elongation is facilitated by a family of seven enzymes called elongases (elongation of very long chain fatty acids 1-7 ELOVL 1-7).(24) ELOVL, similarly to CerS

have broad spectrum of substrate specificity depending on length and saturation of fatty acid hydrocarbon chain. They are also tissue specific. A summary of substrate preference, as well as tissue location is included in Table 2.(27) Notably, ELOVL 4, located in epidermis, is the only elongase that can biosynthesize fatty acids with hydrocarbon chains longer than 24 carbons.(24)

Table 2 Summary of substrate preference and tissue location of ELOVL 1-7

Number of ELOVL	Substrate specificity	Tissue location
ELOVL 1	C22 to C24	Ubiquitous
ELOVL 2	C20 to C22	Testis, liver
ELOVL 3	C16 to C22	Hair, sebaceous glands, testis
ELOVL 4	≥ C24	Epidermis, brain, testis, retina
ELOVL 5	C18 to C20	Ubiquitous
ELOVL 6	C12 to C16	Ubiquitous
ELOVL 7	C16 to C20	Prostate, pancreas, kidney

Fatty acids produced by this process are subsequently either immediately entering the synthesis of Cer catalyzed by CerS, or hydroxylated and then entering the synthesis. Hydroxylation occurs on the α- or ω- position of the fatty acid. α-Hydroxylation is somehow unclear. The major enzyme catalyzing α-hydroxylation is the fatty acid 2-hydroxylase (FA2H). This enzyme is upregulated in brain and skin. Although when an FA2H deficiency is noticed in these, there were visible neurodegenerative aberrations, whilst no skin abnormalities. This fact could indicate, existence of an enzyme with a similar function.(24) This enzyme could be phytanoyl-CoA 2-hydroxylase, that can generate α-hydroxylated acyl-CoA chains with length up to 18 carbon atoms *in-vitro*.(24, 33) The other way is ω-hydroxylation, which depends solely on cytochrome P450 family 4 (CYP4F) enzymes, particularly CYP4F22.(34) ω-Hydroxyl fatty acids are then esterified by a linoleic acid (C18:2-COOH) in 95% of cases. Ester synthesis is catalyzed by ω-acyltransferase activity facilitated by patatin-like phospholipase 1 (PNPLA 1).(35, 36)

3.5. Skin diseases connected with skin Cer alteration

Numerous skin disorders have been connected with alterations in Cer levels or their composition in the human skin epidermis. AD (21) and psoriasis have been causally linked with these epidermal changes.(16, 20, 23) Many more disorders have been discussed with the ceramide abnormalities over the years.(23)

3.5.1. Atopic Dermatitis

AD, also known as atopic eczema, is characterized by chronic, periodically recurring inflammation of skin. Symptoms of AD include itchy erythema combined with scaly and hyper keratinized skin.(37) The AD symptoms are developed during early childhood (in 60% of patients in the first year of life) and usually go into remission by adolescence.(38) Most common affected areas in infants include cheeks, scalp, trunk and extremities. As an individual gets to early childhood, flexural areas get affected. In adults, hands and feet are usually affected.(39) Complications as asthma or allergic rhinitis occur below 5 years of age in 85% of cases. Prevalence of AD worldwide is up to 20% in children and the symptoms proceed to adult age in 1% to 3% of cases. The number of cases increases each year.(38)

Even though, pathogenesis of AD is multifactorial and includes e.g., environmental factors, allergic reaction, immunity system dysfunction or mutation in filaggrin gene,(39) it has been reported, that there is a significant difference in SC ceramide levels and composition between healthy skin and skin diseased with AD.(40, 41) The studies have shown a significant decrease of Cer[EOS] in skin with AD. In general, the diseased skin showed decreased levels of Cer with sidechains longer than 50 carbon atoms in total, at the expense of Cer with sidechains shorter than 40 carbon atoms in total.(16) There was a connection between Cer composition change and decrease of SC barrier function. Shortening of Cer sidechains leads to irregular lipids' folding, increased levels of TEWL, and increased disease severity.(22)

Based on the fact, that Cer levels and composition are altered, there are more explanations to this matter. Logical approach is to look at enzyme activity in AD affected skin. Most of these enzymes were mentioned in chapter 3.4. Decrease of elongases, especially ELOVL1 and ELOVL 4, has been observed in model murine AD skin. This leads to reduced lengths of Cer and free fatty acids.(42) Decrease in CerS 3, as the crucial enzyme for biosynthesis of long chain Cer, led to lethal skin alteration in mice and complete deficiency of Cer with ≥26 carbon atom chain length.(43) It has been discussed, that

extensive degradation of Cer to a sphingoid base and a fatty acid maintained by ceramidases (observed in AD), leads to accumulation of sphingosine-1-phosphate. Sphingosine-1-phosphate could trigger release of tumor necrosis factor alpha (TNF-α) and interleukin 8 (IL-8), and thus promote inflammation in skin.(44)

AD severity is diagnosed by a clinical tool called scoring atopic dermatitis (SCORAD) evaluating area affected by lesions, intensity of the lesion area and subjective symptoms mainly itch and sleeplessness (scale from 0 for no itch to 10 for the worst itch).(45) TEWL has proven to be a comparable indicator to SCORAD in AD disease activity.(46)

Treatment of AD includes emollients, topical and systemic corticosteroids, calcineurin inhibitors, phototherapy and many more options depending on an acuteness of the disease.(47)

3.5.2. Psoriasis

Psoriasis is a non-contagious genetically mediated autoimmune skin disease that is characterized by scaly erythematous plaques. Plaques are sharply circumscribed and could be scattered on small areas of the body or affect large body areas. Most common areas are forearms, shins or scalp, but it can occur in any skin area. It can be divided to 5 groups (plaque, eruptive, inverse, pustular and erythrodermic psoriasis), of which the plaque psoriasis is the most common with prevalence over 90% of all cases of psoriasis.(48) Prevalence of psoriasis in North America and Europe is about 2%(49), while up to 80% of cases are mild and lesions are controlled relatively easily by topical therapy.(50) Psoriasis is a chronic disease with acute exacerbations triggered by multiple factors such as sunburn, chemical irritation, mild mechanical trauma (scratches or tattoos) or various drugs(51) (non-steroidal anti-inflammatory drugs, β-blockers, lithium).(48)

Unlike AD, there was no significant decrease of overall Cer levels in psoriasis. However, change in specific Cer content has been observed. First, Cer containing phytosphingosine in their structure, specifically Cer[AP] and Cer[NP], decreased by 27% and 66% respectively compared to healthy SC. On the other hand, Cer[AS] and Cer[NS] have shown comparable increase.(52)

Similar change to AD is the decrease of Cer[EOS]. Compared to healthy SC, there was a 40% decrease of this Cer.(51) Cer[EOS] is an ultra-long Cer, that has proven to be a key part in water retention and decrease of TEWL. The importance of Cer[EOS] is described

by the presence of linoleate moiety in the molecule, which gives the molecule its vital attributes.(53)

Treatment of psoriasis, being similar to AD, includes emollients, keratolytic agents, coal tar, topical corticosteroids, phototherapy, peroral drugs (corticosteroids, methotrexate, cyclosporine) and phototherapy. There is no effective cure for psoriasis yet, and all treatment methods serve only to relieve from symptoms.(54)

3.5.3. Cer substitution therapy of skin diseases

Treatment of AD and psoriasis requires complex and individual approaches as mentioned before. The use of topical or even systemic corticosteroids is though inevitable in many cases. This fact has many negative adverse effects in systemic (especially) but also topical application of corticosteroids. Therefore, the treatment of these skin diseases aims to minimize the usage of these drugs. One of the ways to minimize it, is skin hydration and moisturizing. Among others, Cer supplementation is being extensively investigated for this matter. Many studies have proven improvements in disease severity and also reduction of corticosteroid therapy in the course of AD and psoriasis.(55-57) In addition the Cer therapy exhibited little to no adverse effects.(56) Usage of Cer-rich emollients have shown decrease of TEWL, restoration of permeation skin barrier, facilitated protection against external irritants, and thus prevention of the inflammation.(55, 57)

A study has shown, that combination of Cer[EOS] and Cer[NP] in an emulsion applied topically improves skin hydration and decreases TEWL in sodium lauryl sulfate treated skin.(16) Another study has tested emollient foam combining Cer and hyaluronic acid, compared to 1% pimecrolimus cream, monitoring improvement in patients with AD flare up. Results of this study have shown significant efficiency in treatment of mild or moderate AD. As for the emollient foam, 82% of treated lesions were evaluated clear after 4 weeks of treatment, compared to 71% in the pimecrolimus cream.(58) A ceramide-dominant, physiological lipid-based emollient has been used replacing standard emollient therapy along with the standard AD therapy (corticosteroids and tacrolimus applied topically). This therapy alteration led to decreased levels of TEWL in correlation with SCORAD values. In addition, TEWL values kept decreasing, even after SCORAD values plateaued. Overtime, slow but noteworthy improvement was visible also in SC cohesion and hydration.(46)

3.6. Pseudoceramides

pCer are synthetic molecules mimicking the structure of Cer found in human SC. They maintain the small polar head in a form of tertiary amine or an amide bond, as well as one or multiple hydroxyl groups. This polar head is accompanied by two long acyl chains of various length as a hydrophobic part of the molecule.(16) The reason for inventing pCer is to find molecules that could act like endogenous Cer, but with better affordability and simplicity of synthesis.(59)

pCer have proven to maintain a similar behavior compared to true Cer.(16) Their supplementation in essential fatty acid deficient rat skin has improved the skin barrier function similarly to Cer.(60) Treating AD skin with pCer lotion resulted in reducing of skin symptoms, as well as in increase of water content and decrease of TEWL. Accumulated levels of pCer were similar to endogenous Cer switching the ceramide profile to the one of healthy skin.(61) A pCer derived from serine has been synthesized. This Cer analogue is structurally similar to Cer[NS], replacing allylic hydroxyl by an ester bond.(59) The barrier-repairing ability of this molecule was evaluated and showed a significant improvement of damaged SC barrier properties. This ability was described by a physico-chemical action of the molecule in SC.(59, 62) pCer have also proven to be an appropriate vehicle for topical corticosteroid delivery. Topical corticosteroids are known to cause an impairment of SC permeability barrier, by decreasing the synthesis of lipids in epidermis. A lipid mixture containing pCer was used to deliver a mid-potency corticosteroid to perturbed (oxazolone-induced) murine model skin. This mixture was compared to PG/EtOH vehicle. Delivering the corticosteroid by the lipid mixture resulted in superior anti-inflammatory effect of the corticosteroid with a better safety profile, since the lipid mixture speeded up the reparation of SC barrier function, partially negating the adverse effect of the corticosteroid.(55)

3.7. Fluorocarbon chemistry and medicinal use

Fluorine is the most electronegative atom in the periodic table of elements. Due to the difference in electronegativity, the C-F bond is unreactive and strongly polarized. Also, these two atoms create the strongest single bond in organic chemistry. Fluorine has similar size to a hydrogen atom and can be substituted in a hydrocarbon molecule without significantly changing the size of the molecule. However, the substitution of hydrogen by fluorine alters the properties of organic molecules, which are often incomparable to properties of non-fluorinated molecules. This might be the reason why fluorocarbons are widely used in medicine, chemical biology, agrochemicals, material chemistry and many more areas.(63) In fact, 20% of used drugs contain fluorine and this number is even higher in agrochemicals (approximately 30%).(64) One of the unique properties of fluorocarbon is that when an organic molecule is fluorinated to a higher extent it becomes hydrophobic but also lipophobic, it becomes so-called fluorophilic. This means, that solubility is limited in water or most organic solvents except the fluorinated ones.(63)

As mentioned earlier, many of the fluorocarbon properties are used in medicine. Perfluorocarbons are inert compounds with low toxicity, high vapor pressure and low viscosity and friction. They are used as gas delivery carriers, due to their high affinity for gas molecules, also as drug delivery systems for inhalation. They are used as blood substitutes or contrast substances for ultrasound imaging.(64)

To the best of our knowledge, polyfluorinated pCer have not been reported yet. However, when polyfluorination was performed on a known permeation enhancer, it led to a complete abolishment of permeation enhancing ability. This fact could be explained by insufficient disruption of lipid bilayer in skin by the polyfluorinated molecule.(65) In addition, a skin exposure reduction paste against chemical warfare agents (SERPACWA) has been patented and used complementarily to protecting suits for the army of United States. This paste contains a 1:1 mixture of polytetrafluoroethylene and perfluoroalkyl polyether(66) and has proven to serve for simple but effective skin protection against chemical agents.(67) Longer fluorinated acyl chains exhibit hydrophobic but also lipophobic attributes. Thus, compounds bearing both alkyl and polyfluoroalkyl chains may increase rigidity of the SC lipids.(65)

4. Experimental part

4.1. Chemicals, materials, and instruments

All chemicals were purchased from Sigma-Aldrich (Schnelldorf, Germany), Merck (Darmstadt, Germany), Lach-Ner (Neratovice, Czech Republic), PENTA (Prague, Czech Republic), and 1H,1H,2H,2H-perfluorotetradecan-1-ol was purchased from Apollo Scientific Ltd. (Stockport, United Kingdom). Silica gel 60 F254 plates were used for TLC and silica gel 60 (230-400 mesh) was used for column chromatography. Both were purchased from Merck (Darmstadt, Germany). Potassium permanganate solution [mixture of $KMnO_4$ (1.5 g), K_2CO_3 (10 g), 10% NaOH (1.25 ml) and H_2O (200 ml)] was used for detection (immersion of TLC plate and heating to 80-100 ºC). NMR spectroscopy was used for compound characterization. As instrumentation Varian mercury Vx BB 300 (^1H at 300 MHz and ^{13}C at 75.5 MHz) or Varian VNMR S500 (^1H at 500 MHz and ^{13}C at 125 MHz) were used, using tetramethyl silane as an internal standard. NMR spectra were further evaluated in MestReC and MestReNova software. Mass spectra were measured at Expression CMS in connection with ASAP®, Advion, Inc. (USA) using APCI source of ionization. Melting points were measured by Buchi B-540 melting point apparatus. For infrared spectroscopy a Nicolet 6700 FT-IR instrument was used. Samples were measured in the range of 400-4000 cm^{-1}, at 25 ºC, with 128 scans, using a crystal of Germanium. Skin was dermatomed to final thickness of 500 µm using Acculant 3Ti (Aesculap, Center Valley, PA, USA). AquaFlux AF 200 instrument (Biox Systems Ltd, UK) was used for TEWL measurement. Electric impedance (EI) was measured using LCR meter 4080 (Conrad Electronic, Hirschau, Germany). A Shimadzu Prominence instrument was used for high pressure liquid chromatography (HPLC) with a LiChroCART 250-4 column (LiChrospher 100 RP-18, 5 µm, Merck, Darmstadt, Germany). Chemical formulas and structures were created using ChemDraw Professional software and statistical data were evaluated in GraphPad Prism software.

4.2. Synthesis

4.2.1. Synthesis scheme

All final molecules were synthesized following a general synthetic protocol of four steps.

The first step was an ester synthesis reaction of *O*-benzyl-*N*-(*tert*-butyloxycarbonyl)-L-serine with the desired alcohol. The second step was a selective removal of *tert*-butyloxycarbonyl (Boc) group. The third step was an amidation reaction with lignoceric acid and the fourth step was Benzyl (Bn) group deprotection which is providing the final molecules. The schematic procedure is shown in Figure 8 and a detailed general procedure with the specific conditions for each step is following.

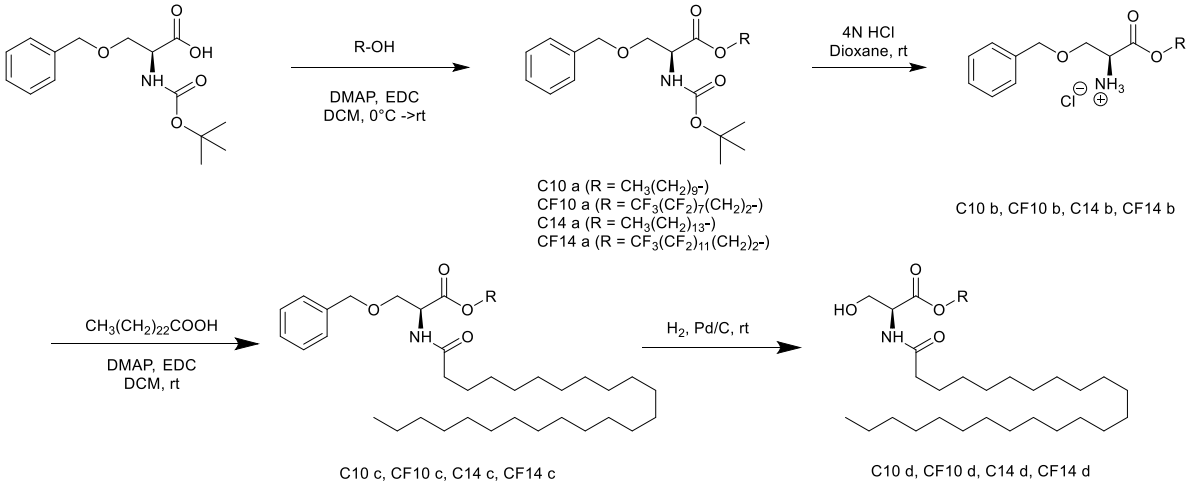

Figure 8 Synthesis scheme

4.2.2. General procedures

4.2.2.1. General procedure for the first step (ester synthesis)

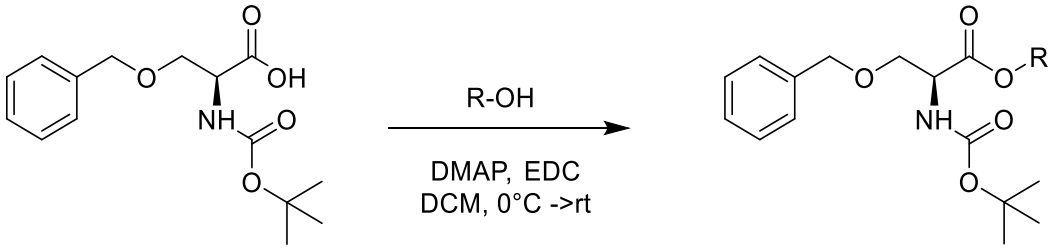

Figure 9 General scheme for ester synthesis

O-benzyl-*N*-(*tert*-butyloxycarbonyl)-L-serine (1 eq.) was dissolved in the minimum volume of dichloromethane (DCM) and the reaction mixture was cooled to 0 ºC using an ice bath. Afterwards, 4-dimethylaminopyridine (DMAP) (0.1 eq.), 1-ethyl-3-(3-dimethylaminopropyl)-carbodiimide (EDC) (1.3 eq.) and the desired alcohol (1.5 eq.) were

added to the reaction vessel. The reaction mixture was stirred at 0 ºC for 2 hours and at room temperature for 22 hours. After the reaction completion (checked by TLC, see below) the mixture was diluted with DCM until the volume was doubled and washed with the same volume of saturated solution of $NaHCO_3$ (3x). The organic phase was dried over Na_2SO_4, filtered through a filter paper and the organic solvent was evaporated under reduced pressure at rotary evaporator. Pure product was obtained by a column chromatography using the eluent specified separately for each product.

4.2.2.2. General procedure for the second step (Boc-deprotection)

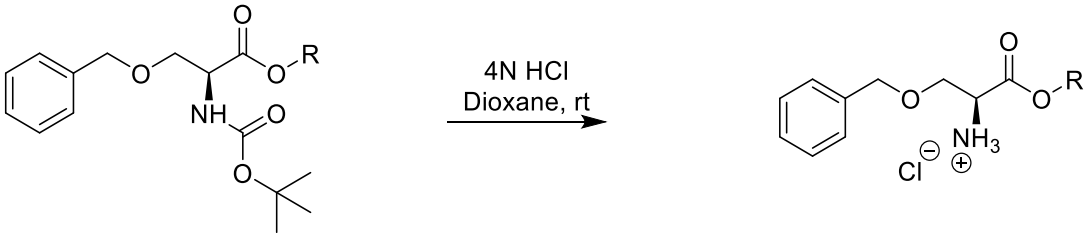

Figure 10 General scheme for Boc deprotection

The starting material was loaded in a flask under nitrogen. A solution of 4N HCl (amount specified for each reaction) in dioxane was added and the reaction mixture was monitored every 30 minutes by TLC. When no starting material was detected, the solvent was evaporated under reduced pressure at rotary evaporator while diethyl ether (10 ml) and *n*-hexane (10 ml) were added and evaporated repeatedly at rotary evaporator under reduced pressure (3 cycles). The product was further dried in high vacuum and used for next reaction.

4.2.2.3. General procedure for the third step (amidation)

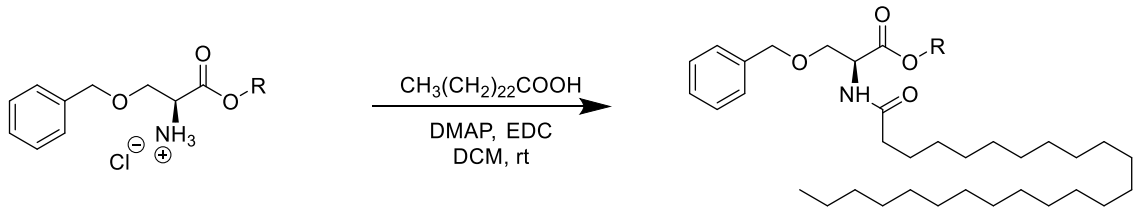

Figure 11 General scheme for amidation

The hydrochloric acid salt prepared above (1.0 eq) was suspended in a volume of DCM specified separately for each reaction and dissolved after DMAP (1.1 eq.) was added. EDC (1 eq.) and lignoceric acid (1 eq.) were also added to the mixture and the reaction allowed to stir at room temperature overnight. The reaction mixture was then diluted with DCM until the volume was doubled and washed with the same volume of saturated solution of $NaHCO_3$ (3x). The organic phase was then dried over Na_2SO_4, filtered through a filter

paper and the organic solvent was evaporated under reduced pressure at rotary evaporator. The pure product was obtained by a column chromatography using the eluent specified separately for each product.

4.2.2.4. General procedure for the fourth step (Bn-deprotection)

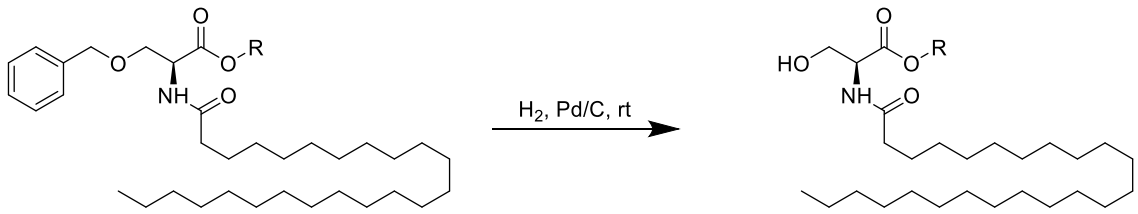

Figure 12 General scheme for Bn deprotection

Pd/C (amount specified in each reaction) was put in a flask with a stirrer, evacuated and refilled with nitrogen (3x). Methanol was added in the flask and the flask was again evacuated and refilled with nitrogen. Afterwards the starting material (1 eq.) was dissolved in the appropriate solvent (specified differently for each case) and the solution was added to the flask. The flask was then evacuated and refilled with hydrogen (3x). The reaction was kept under H_2 atmosphere while monitored by TLC. After no starting material was detected, the reaction mixture was filtered through a double filter paper, and the solvent was evaporated under reduced pressure at rotary evaporator.

4.2.3. Synthesis of individual compounds

4.2.3.1. Synthesis of decyl *O*-benzyl-*N*-(*tert*-butoxycarbonyl)-L-serinate (C10 a)

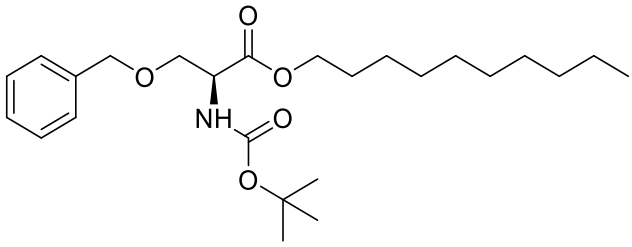

Figure 13 Structure of decyl O-benzyl-N-(tert-butoxycarbonyl)-L-serinate

The compound was synthesized according to the general procedure described at 4.2.2.1. 1000 mg of *O*-benzyl-*N*-(*tert*-butyloxycarbonyl)-L-serine (3.39 mmol, 1.0 eq.), 41 mg of DMAP (0.34 mmol, 0.1 eq.), 778 µl of EDC (4.40 mmol, 1.3 eq.) and 968 µl of 1-decanol (5.07 mmol, 1.5 eq.) were used. The mobile phase for column chromatography was a mixture of *n*-hexane/EtOAc (10/1). R_f = 0.30 in *n*-hexane/EtOAc (10/1). 854 mg of the desired compound were isolated (yield = 58%) as a yellowish oily substance. MS calculated

for $C_{25}H_{41}NO_5$ = 435.3, MS found = 436.6 $(M+H)^+$. ^{1}H-NMR ($CDCl_3$, 500 MHz) δ/ppm: 0.80 (t, 3H, J = 6.9 Hz), 1.15-1.25 (m, 14H), 1.37 (s, 9H), 1.49-1.59 (m, 2H), 3.61 (dd, 1H, J = 9.3 Hz, J = 3.3 Hz), 3.80 (dd, 1H, J = 9.3 Hz, J = 3.3 Hz), 4.06-4.11 (m, 2H), 4.35 (dt, 1H, J = 8.9 Hz, 3.3 Hz), 4.40 (d, 1H, J = 12.2 Hz), 4.47 (d, 1H, J = 12.2 Hz), 5.32 (d, 1H, 8.9 Hz), 7.16-7.28 (m, 5H). ^{13}C NMR ($CDCl_3$, 125 MHz) δ 170.87, 155.64, 137.75, 128.52, 127.90, 127.68, 80.00, 73.40, 70.30, 65.81, 54.21, 32.01, 29.67, 29.63, 29.43, 29.36, 28.69, 28.46, 25.95, 22.81, 14.24. IR (ATR): 3649, 2926, 2856, 1717, 1647, 1498, 1455, 1392, 1366, 1340, 1296, 1247, 1201, 1164, 1062, 1028 cm^{-1}.

4.2.3.2. Synthesis of (S)-3-(benzyloxy)-1-(decyloxy)-1-oxopropan-2-aminium chloride (C10 b)

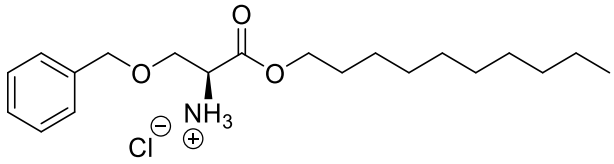

Figure 14 Structure of (S)-3-(benzyloxy)-1-(decyloxy)-1-oxopropan-2-aminium chloride

The compound was synthesized according to the general procedure for Boc deprotection described at 4.2.2.2 using 373 mg of decyl *O*-benzyl-*N*-(*tert*-butoxycarbonyl)-L-serinate (0.81 mmol, 1 eq.) and 5 ml of 4N HCl in dioxane (20 mmol, 25 eq.). The total reaction time was 1 hour. The mobile phase for TLC control was a mixture of *n*-hexane/EtOAc (10/1). 306 mg of the desired product were isolated (yield = 96%) as yellowish crystals, mp = 90 ºC. MS calculated for $C_{20}H_{34}NO_3$ = 336.3, MS found = 337.3 $(M+H)^+$. ^{1}H-NMR ($CDCl_3$, 500 MHz) δ/ppm: 0.88 (t, 3H, J = 7.1 Hz), 1.19-1.32 (m, 14H), 1.53-1.60 (m, 2H), 3.96 (d, 1H, J = 10.2 Hz, 4.04-4.20 (m, 3H), 4.36 (s, 1H), 4.48 (d, 1H, J = 12.1 Hz), 4.70 (d, 1H, J = 12.1 Hz), 7.20-7.35 (m, 5H), 8.86 (s, 3H). ^{13}C NMR ($CDCl_3$, 125 MHz) δ 167.51, 137.31, 128.46, 127.93, 127.87, 73.49, 67.14, 66.97, 53.67, 32.00, 29.67, 29.61, 29.42, 29.32, 28.44, 25.81, 22.79, 14.22. IR (ATR): 2922, 2853, 2656, 1737, 1586, 1503, 1467, 1453, 1413, 1395, 1357, 1330, 1309, 1248, 1235, 1160, 1136, 1111, 1088, 1073. 1027, 735 cm^{-1}.

4.2.3.3. Synthesis of decyl-*O*-benzyl-*N*-tetracosanoyl-L-serinate (C10 c)

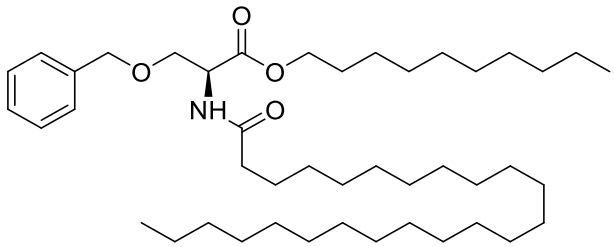

Figure 15 Structure of decyl O-benzyl-N-tetracosanoyl-L-serinate

The compound was synthesized according to the general procedure for amidation described at 4.2.2.3. 534 mg of (S)-3-(benzyloxy)-1-(decyloxy)-1-oxopropan-2-aminium chloride (1.44 mmol, 1 eq.), 529 mg of lignoceric acid (1.44 mmol, 1 eq.), 155 µl of EDC (1.44 mmol, 1 eq.), 193 mg of DMAP (1.58 mmol, 1.1 eq.). Mobile phase for column chromatography was *n*-hexane/EtOAc (7/1, later changed to 5/1). R_f = 0.30 in *n*-hexane/EtOAc (7/1). 432 mg of the desired product were isolated (yield = 44%) as white crystals, mp = 75-76 ºC. MS calculated for $C_{44}H_{79}NO_4$ = 685.6, MS found = 686.9 $(M+H)^+$. ^{1}H-NMR ($CDCl_3$, 500 MHz) δ/ppm: 0.88 (t, 3H, J = 6.8 Hz), 1.16-1.38 (m, 54H), 1.55-1.71 (m, 4H), 2.22 (t, 2H, 6.8 Hz), 3.69 (dd, 1H, J = 9.4 Hz, J = 3.1 Hz), 3.90 (dd, 1H, J = 9.4 Hz, J = 3.1 Hz), 4.09-4.18 (m, 2H), 4.48 (d, 1H, J = 12.0 Hz), 4.53 (d, 1H, J = 12.0 Hz), 4.75 (dt, 1H, J = 8.2 Hz, 3.1 Hz), 5.32 (d, 1H, 8.2 Hz), 7.17-7.46 (m, 5H). ^{13}C NMR ($CDCl_3$, 125 MHz) δ 173.06, 170.61, 137.70, 128.57, 127.99, 127.74, 73.45, 70.14, 65.94, 52.68, 36.75, 32.07, 32.03, 29.85, 29.82, 29.80, 29.79, 29.68, 29.65, 29.51, 29.44, 29.40, 29.36, 28.67, 25.96, 25.74, 22.84, 22.82, 14.26. IR (ATR): 3675, 3302, 2918, 2849, 1742, 1642, 1559, 1540, 1497, 1473, 1462, 1398, 1367, 1339, 1236, 1204, 1153, 1092, 1060, 731 cm^{-1}.

4.2.3.4. Synthesis of decyl *N*-tetracosanoyl-L-serinate (C10 d)

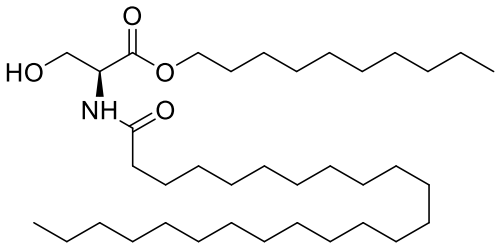

Figure 16 Structure of decyl N-tetracosanoyl-L-serinate

The compound was synthesized according to the general procedure for Bn deprotection described at 4.2.2.4. 37 mg of decyl *O*-benzyl-*N*-tetracosanoyl-L-serinate (0.05 mmol, 1 eq.) was dissolved in 6 ml of EtOAc, 32 mg of Pd/C (0.30 mmol, 6 eq.) was added.

Reaction time was 20 hours. Mobile phase for TLC control was *n*-hexane/EtOAc (3/1). R_f = 0.20 in *n*-hexane/EtOAc. 31 mg of the desired product were isolated (yield = 97%) as white crystals, mp = 83 ºC, MS calculated for $C_{37}H_{73}NO_4$ = 595.6, MS found = 596.9 $(M+H)^+$. ^{1}H-NMR ($CDCl_3$, 500 MHz) δ/ppm: 0.80-0.98 (m, 6H), 1.17-1.44 (m, 54H), 1.60-1.70 (m, 4H), 2.27 (t, 2H, 7.6 Hz), 2.67 (bs, 1H), 3.96 (d, 2H, J = 3.8 Hz), 4.19 (t, 2H, J = 6.7 Hz), 4.68 (dt, 1H, J = 7.2 Hz, J = 3.8 Hz), 6.42 (d, 1H, J = 7.2 Hz). ^{13}C NMR ($CDCl_3$, 125 MHz) δ 173.96, 170.71, 66.29, 64.15, 55.07, 36.70, 32.07, 32.02, 29.85, 29.81, 29.78, 29.66, 29.64, 29.51, 29.49, 29.43, 29.39, 29.33, 28.64, 25.94, 25.72, 22.83, 22.81, 14.26, 14.24. IR (ATR): 3305, 2959, 2917, 2850, 1722, 1698, 1684, 1645, 1559, 1540, 1507, 1473, 1417, 1234, 1211, 1144, 1068, 970, 920, 716 cm^{-1}.

4.2.3.5. Synthesis of 1H,1H,2H,2H-perfluorodecyl tetracosanoyl-L-serinate (CF10 a)

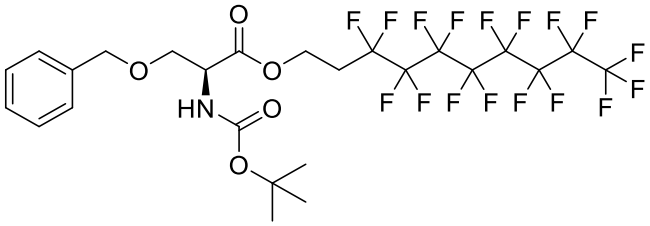

Figure 17 Structure of 1H,1H,2H,2H-perfluorodecyl O-benzyl-N-(tert-butoxycarbonyl)-L-serinate

The compound was synthesized according to the general procedure described at 4.2.2.1. 1000 mg of *O*-benzyl-*N*-(*tert*-butyloxycarbonyl)-L-serine (3.38 mmol, 1.0 eq.), 41 mg of DMAP (0.34 mmol, 0.1 eq.), 778 µl of EDC (4.40 mmol, 1.3 eq.) and 2353 mg 1H,1H,2H,2H-perfluoro-1-decanol (5.07 mmol, 1.5 eq.) were used. The mobile phase for column chromatography was a mixture of *n*-hexane/EtOAc (7/1). R_f = 0.33 in *n*-hexane/EtOAc (7/1). 477 mg of the desired compound were isolated (yield = 21%) as white crystals, mp = 67 ºC, MS calculated for $C_{25}H_{24}F_{17}NO_5$ = 741.1, MS found = 742.3 $(M+H)^+$. ^{1}H-NMR ($CDCl_3$, 500 MHz) δ/ppm: 1.45 (s, 9H), 2.35 (tt, 2H, J = 6.4 Hz, J = 18,1 Hz), 3.68 (dd, 1H, J = 9.4 Hz, J = 3.3 Hz), 3.88 (dd, 1H, J = 9.4 Hz, J = 3.3 Hz), 4.36-4.50 (m, 3H), 4.53 (d, 1H, J = 12.1 Hz), 5.38 (d, 1H, 8.9 Hz), 7.24-7.36 (m, 5H). ^{13}C NMR ($CDCl_3$, 125 MHz) δ 170.52, 155.64, 137.53, 128.57, 128.06, 127.82, 80.27, 73.47, 69.92, 57.36, 54.16, 30.61 (t, 21.9 Hz), 30.44, 28.42. IR (ATR): 3462, 1742, 1716, 1698, 1684, 1647, 1559, 1495, 1458, 1395, 1370, 1360, 1340, 1250, 1198, 1144, 1125, 1082, 1062, 1038, 1029, 964, 849, 776 cm^{-1}.

4.2.3.6. Synthesis of (S)-3-(benzyloxy)-1-((1H,1H,2H,2H-perfluorodecyl)oxy)-1-oxopropan-2-aminium chloride (CF10 b)

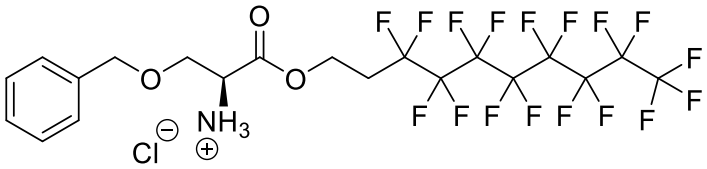

Figure 18 Structure of (S)-3-(benzyloxy)-1-((1H,1H,2H,2H-perfluorodecyl)oxy)-1-oxopropan-2-aminium chloride

The compound was synthesized according to the general procedure described at 4.2.2.2. 368 mg of 1H,1H,2H,2H-perfluorodecyl tetracosanoyl-L-serinate (0.50 mmol, 1 eq.), 5 ml of 4N HCl in dioxane (25 mmol, 50 eq.), Reaction time was 3 hours. The mobile phase for TLC control was a mixture of *n*-hexane/EtOAc (7/1). 300 mg of the desired product were isolated (yield = 89%) as yellowish crystals, mp = 110 ºC. MS calculated for $C_{20}H_{17}F_{17}NO_3^+$ = 642.1, MS found = 642.3. ^{1}H-NMR (CD_3OD, 500 MHz) δ/ppm: 2.49-2.74 (m, 2H), 3.87 (dd, 1H, J = 10.6 Hz, J = 3.0 Hz), 3.95 (dd, 1H, J = 10.6 Hz, J = 4.1 Hz), 4.35 (dd, 1H, J = 4.1 Hz, J = 3.0 Hz), 4.50-4.61 (m, 3H), 4.63 (d, 1H, J = 12.0 Hz), 7.25-7.46 (m, 5H). ^{13}C NMR (CD_3OD, 125 MHz) δ 168.42, 138.33, 129.53, 129.19, 129.18, 74.52, 67.82, 59.50, 54.44, 31.03 (t, 21.1 Hz).. IR (ATR): 3675, 2931, 1743, 1698, 1684, 1654, 1647, 1578, 1559, 1516, 1489, 1455, 1374, 1340, 1199, 1143, 1116, 1073, 957, 801, 748 cm^{-1}.

4.2.3.7. Synthesis of 1H,1H,2H,2H-perfluorodecyl-*O*-benzyl-*N*-tetracosanoyl-L-serinate (CF10 c)

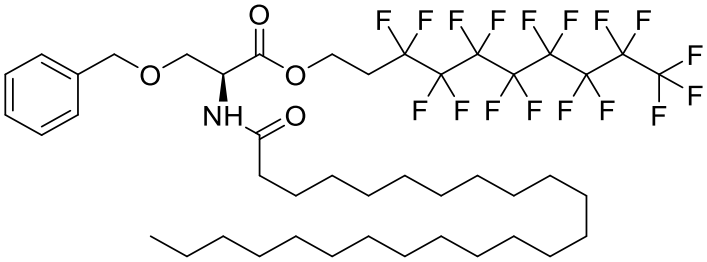

Figure 19 Structure of 1H,1H,2H,2H-perfluorodecyl O-benzyl-N-tetracosanoyl-L-serinate

The compound was synthesized according to the general procedure for amidation described at 4.2.2.3. 276 mg of (S)-3-(benzyloxy)-1-(1H,1H,2H,2H-perfluorodecyloxy)-1-oxopropan-2-aminium chloride (0.41 mmol, 1 eq.), 149 mg of lignoceric acid (0.41 mmol, 1 eq.), 72 µl of EDC (0.41 mmol, 1 eq.), 50 mg of DMAP (0.45 mmol, 1.1 eq.). Mobile phase for column chromatography was $CHCl_3$. R_f = 0.43 in $CHCl_3$. 292 mg of the desired product were isolated (yield = 72%) as white crystals, mp = 89 ºC. MS calculated for $C_{44}H_{62}F_{17}NO_4$ = 991.4, MS found = 992.7 $(M+H)^+$. ^{1}H-NMR ($CDCl_3$, 500 MHz) δ/ppm:

0.88 (t, 3H, J = 6.9 Hz), 1.2 -1.40 (m, 42H), 1.58-1.68 (m, 2H), 2.22 (t, 2H, J = 6.8 Hz), 2.35 (tt, 2H, J = 6,5 Hz, J = 18,2 Hz), 3.67 (dd, 1H, J = 9.4 Hz, J = 3.1 Hz), 3.90 (dd, 1H, J = 9.4 Hz, J = 3.1 Hz), 4.38-4.49 (m, 3H), 4.51 (d, 1H, J = 12.1 Hz), 4.78 (dt, 1H, J = 8.3 Hz, J = 3.1 Hz), 6.4 (d, 1H, J = 8.3 Hz), 7.17-7.42 (m, 5H). ^{13}C NMR (CDCl3, 125 MHz) δ 173.19, 170.20, 137.47, 128.61, 128.15, 127.88, 73.49, 69.73, 57.46, 52.56, 36.66, 32.08, 30.58 (t, 21.3 Hz), 29.86, 29.81, 29.79, 29.65, 29.51, 29.39, 25.68, 22.84, 14.25. IR (ATR): 3665, 2918, 2850, 1771, 1748, 1734, 1715, 1698, 1688, 1684, 1680, 1647, 1559, 1539, 1517, 1507, 1498, 1490, 1473, 1463, 1458, 1455, 1417, 1362, 1339, 1201, 1148, 1117, 1056, 730 cm^{-1}.

4.2.3.8. Synthesis of 1H,1H,2H,2H-perfluorodecyl tetracosanoyl-L-serinate (CF10 d)

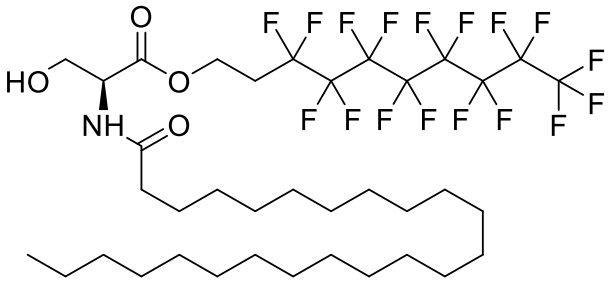

Figure 20 Structure of 1H,1H,2H,2H-perfluorodecyl tetracosanoyl-L-serinate

The compound was synthesized according to the general procedure for Bn deprotection described at 4.2.2.4. 108 mg of 1H,1H,2H,2H-perfluorodecyl *O*-benzyl-*N*-tetracosanoyl-L-serinate (0.10 mmol, 1 eq.) was dissolved in a mixture of MeOH/$CHCl_3$ (2/1), 53 mg of Pd/C (0.50 mmol, 5 eq.) was added. Reaction time was 24 hours. Mobile phase for TLC control was *n*-hexane/EtOAc (4/1). R_f = 0.08 in *n*-hexane/EtOAc (4/1). 97 mg of the desired product were isolated (yield = 99%) as white crystals, mp = 110 ºC. MS calculated for $C_{37}H_{56}F_{17}NO_4$ = 901.4, MS found = 902.7 $(M+H)^+$. ^{1}H-NMR ($CDCl_3$, 500 MHz) δ/ppm: 0.81 (t, 3H, J=6.8Hz), 1.18-1.26 (m, 40H), 1.48-1.58 (m, 2H), 2.19-2.25 (m, 2H), 2.52-2.55 (m, 2H), 4.09-4.15 (m, 3H), 4.40-4.50 (m, 2H). Due to low solubility of the compound, signals with expected ppm were found, but the integration and coupling constants could not be evaluated precisely. Also, the carbon NMR could not be measured. However, the MS confirmed the mass of the final compound. IR (ATR): 3536, 3357, 2917, 2850, 1734, 1651, 1558, 1522, 1473, 1417, 1356, 1330, 1309, 1200, 1145, 1132, 1114, 1099, 1045, 999, 716 cm^{-1}.

4.2.3.9. Synthesis of tetradecyl *O*-benzyl-*N*-(*tert*-butoxycarbonyl)-L-serinate (C14 a)

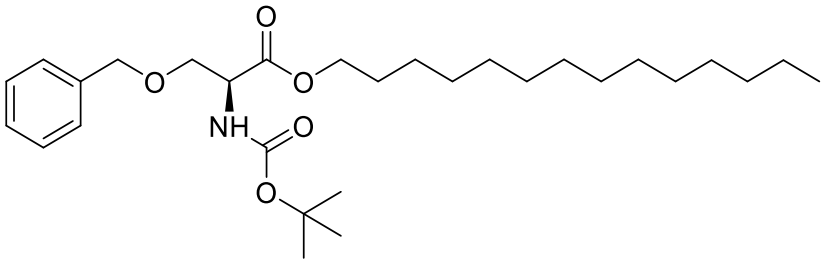

Figure 21 Structure of tetradecyl O-benzyl-N-(tert-butoxycarbonyl)-L-serinate

The compound was synthesized according to the general procedure described at 4.2.2.1. 500 mg of *O*-benzyl-*N*-(*tert*-butyloxycarbonyl)-L-serine (1.69 mmol, 1.0 eq.), 21 mg of DMAP (0.17 mmol, 0.1 eq.), 389 µl of EDC (2.20 mmol, 1.3 eq.) and 545 mg tetradecanol (2.54 mmol, 1.5 eq.) were used. The mobile phase for column chromatography was a mixture of *n*-hexane/EtOAc (9/1). R_f = 0.35 in *n*-hexane/EtOAc (9/1). 389 mg of the desired compound were isolated (yield = 47%) as white crystals, mp = 36 ºC. MS calculated for $C_{29}H_{49}NO_5$ = 491.4, MS found = 492.6 $(M+H)^+$. ^{1}H-NMR ($CDCl_3$, 500 MHz) δ/ppm: 0.88 (t, 3H, J = 6.9 Hz), 1.20-1.37 (m, 22H), 1.45 (s, 9H), 1.56-1.65 (m, 2H), 3.69 (dd, 1H, J = 9.4 Hz, J = 3.3 Hz), 3.88 (dd, 1H, J = 9.4 Hz, J = 3.3 Hz), 4.07-4.19 (m, 2H), 4.42 (dt, 1H, J = 9.0 Hz, 3.3 Hz), 4.48 (d, 1H, J = 12.3 Hz), 4.54 (d, 1H, J = 12.3 Hz), 5.39 (d, 1H, 9.0 Hz), 7.21-7.41 (m, 5H). ^{13}C NMR ($CDCl_3$, 125 MHz) δ 170.87, 155.64, 137.77, 128.53, 127.91, 127.69, 80.01, 73.41, 70.32, 65.82, 54.22, 32.07, 29.83, 29.81, 29.79, 29.73, 29.65, 29.50, 29.37, 28.70, 28.47, 25.96, 22.83, 14.25. IR (ATR): 3467, 2917, 2850, 1737, 1716, 1698, 1684, 1671, 1647, 1559, 1544, 1497, 1472, 1458, 1369, 1361, 1338, 1254, 1204, 1160, 1125, 1061, 1040, 1030, 999, 963, 924, 893, 855, 775, 736 cm^{-1}.

4.2.3.10. Synthesis of (S)-3-(benzyloxy)-1-oxo-1-(tetradecyloxy)propan-2-aminium chloride (C14 b)

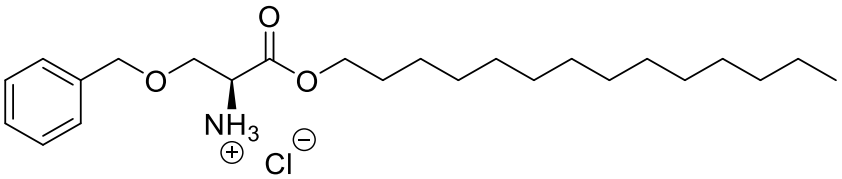

Figure 22 Structure of (S)-3-(benzyloxy)-1-oxo-1-(tetradecyloxy)propan-2-aminium chloride

The compound was synthesized according to the general procedure for Boc deprotection described at 4.2.2.2. 245 mg of tetradecyl *O*-benzyl-*N*-(*tert*-butoxycarbonyl)-L-serinate (0.50 mmol, 1 eq.), 5 ml of 4N HCl in dioxane (25 mmol, 50 eq.). Reaction time

was 2 hours. The mobile phase for TLC control was a mixture of *n*-hexane/EtOAc (10/1). 149 mg of the desired product were isolated (yield = 70%) as yellowish crystals, mp = 87 ºC. MS calculated for $C_{24}H_{42}NO_3^+$ = 392.3, MS found = 392.4. ^{1}H-NMR (CD_3OD, 500 MHz) δ/ppm: 0.87 (t, 3H, J = 7.0 Hz), 1.20-1.38 (m, 22H), 1.55-1.69 (m, 2H), 3.82 (dd, 1H, J = 10.5 Hz, J = 2.9 Hz), 3.92 (dd, 1H, J = 10.5 Hz, J = 2.9 Hz), 4.14-4.20 (m, 1H), 4.22-4.27 (m, 2H), 4.52 (d, 1H, J = 12.0 Hz), 4.62 (d, 1H, J = 12.0 Hz), 7.25-7.38 (m, 5H). ^{13}C NMR (CD_3OD, 125 MHz) δ 168.62, 138.41, 129.55, 129.15, 129.09, 74.51, 68.09, 67.75, 54.48, 33.06, 30.78, 30.75, 30.69, 30.61, 30.46, 30.31, 29.58, 26.85, 23.72, 14.43. IR (ATR): 3650, 2918, 2851, 2136, 1752, 1736, 1698, 1684, 1569, 1464, 1458, 1455, 1374, 1358, 1313, 1228, 1163, 1119, 1089, 1066, 1027, 966, 916, 839, 816, 787, 735 cm^{-1}.

4.2.3.11. Synthesis of tetradecyl *O*-benzyl-*N*-tetracosanoyl-L-serinate (C14 c)

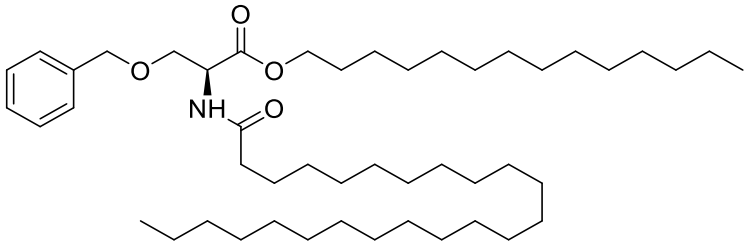

Figure 23 Structure of tetradecyl O-benzyl-N-tetracosanoyl-L-serinate

The compound was synthesized according to the general procedure for amidation described at 4.2.2.3. 127 mg of (S)-3-(benzyloxy)-1-(tetradecyloxy)-1-oxopropan-2-aminium chloride (0.30 mmol, 1 eq.), 110 mg of lignoceric acid (0.30 mmol, 1 eq.), 53 µl of EDC (0.30 mmol, 1 eq.), 40 mg of DMAP (0.33 mmol, 1.1 eq.). Mobile phase for column chromatography was *n*-hexane/EtOAc (7/1). R_f = 0.30 in *n*-hexane/EtOAc (7/1). 104 mg of the desired product were isolated (yield = 47%) as white crystals, mp = 72 ºC. MS calculated for $C_{48}H_{87}NO_4$ = 741.7, MS found = 742.9 $(M+H)^+$. ^{1}H-NMR ($CDCl_3$, 500 MHz) δ/ppm: 0.88 (t, 3H, J = 6.8 Hz), 1.17-1.35 (m, 62H), 1.55-1.67 (m, 4H), 2.22 (t, 2H, 6.8 Hz), 3.69 (dd, 1H, J = 9.4 Hz, J = 3.1 Hz), 3.90 (dd, 1H, J = 9.4 Hz, J = 3.1 Hz), 4.09-4.18 (m, 2H), 4.48 (d, 1H, J = 12.2 Hz), 4.53 (d, 1H, J = 12.2 Hz), 4.75 (dt, 1H, J = 8.2 Hz, 3.1 Hz), 6.27 (d, 1H, 8.2 Hz), 7.22-7.39 (m, 5H). ^{13}C NMR ($CDCl_3$, 125 MHz) δ 173.06, 170.61, 137.71, 128.57, 127.99, 127.74, 73.45, 70.15, 65.94, 52.68, 36.75, 32.07, 29.85, 29.82, 29.80, 29.74, 29.66, 29.51, 29.40, 29.37, 28.68, 25.96, 25.74, 22.84, 14.26. IR (ATR): 3508, 2917, 2849, 1741, 1642, 1539, 1473, 1463, 1366, 1337, 1236, 1204, 1152, 1092, 1059, 1024, 809, 730 cm^{-1}.

4.2.3.12. Synthesis of tetradecyl tetracosanoyl-L-serinate (C14 d)

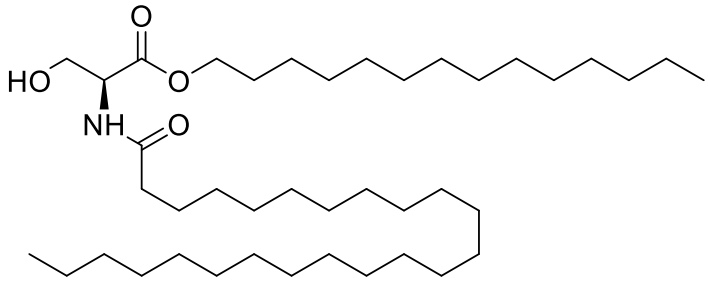

Figure 24 Structure of tetradecyl tetracosanoyl-L-serinate

The compound was synthesized according to the general procedure for Bn deprotection described at 4.2.2.4. 84 mg of tetradecyl *O*-benzyl-*N*-tetracosanoyl-L-serinate (0.11 mmol, 1 eq.) was dissolved in 15 ml of EtOAc, 60 mg of Pd/C (0.56 mmol, 5 eq.) was added. Reaction time was 24 hours. Mobile phase for TLC control was *n*-hexane/EtOAc (3/1). R_f = 0.20 in *n*-hexane/EtOAc (3/1). 62 mg of the desired product were isolated (yield = 85%) as white crystals, mp = 85 ºC. MS calculated for $C_{41}H_{81}NO_4$ = 651.6, MS found = 652.8 $(M+H)^+$. ^{1}H-NMR ($CDCl_3$, 500 MHz) δ/ppm: 0.89 (t, 6H, J = 6.9 Hz), 1.20-1.41 (m, 62H), 1.61-1.71 (m, 4H), 2.27 (t, 2H, 7.6 Hz), 2.62 (bs, 1H), 3.96 (t, 2H, J = 3.8 Hz), 4.19 (t, 2H, J = 6.7 Hz), 4.68 (dt, 1H, J = 7.3 Hz, J = 3.8 Hz), 6.41 (d, 1H, J = 7.3 Hz). ^{13}C NMR ($CDCl_3$, 125 MHz) δ 172.95, 169.71, 65.30, 63.18, 54.08, 35.70, 31.08, 28.86, 28.82, 28.80, 28.78, 28.72, 28.65, 28.64, 28.51, 28.50, 28.40, 28.35, 27.65, 24.94, 24.72, 21.84, 13.26. IR (ATR): 3488, 3304, 2959,2916, 2850, 1722, 1645, 1541, 1472, 1416, 1234, 1211, 1197, 1070, 963, 925, 816, 716 cm^{-1}.

4.2.3.13. Synthesis of 1H,1H,2H,2H-perfluorotetradecyl *O*-benzyl-*N*-(*tert*-butoxycarbonyl)-L-serinate (CF14 a)

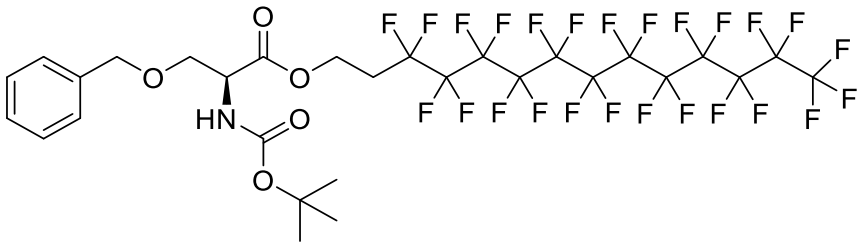

Figure 25 Structure of 1H,1H,2H,2H-perfluorotetradecyl O-benzyl-N-(tert-butoxycarbonyl)-L-serinate

The compound was synthesized according to the general procedure described at 4.2.2.1. 95 mg of *O*-benzyl-*N*-(*tert*-butyloxycarbonyl)-L-serine (0.32 mmol, 1.0 eq.), 4 mg of DMAP (0.03 mmol, 0.1 eq.), 74 µl of EDC (0.42 mmol, 1.3 eq.) and 255 mg 1H,1H,2H,2H-perfluoro-1-tetradecanol (0.38 mmol, 1.2 eq.) were used. The mobile phase

for column chromatography was a mixture of *n*-hexane/$CHCl_3$/EtOAc (4/4/0.8). R_f = 0.33 in *n*-hexane/$CHCl_3$/EtOAc (4/4/0.8). 128 mg of the desired compound were isolated (yield = 43%) as white crystals, mp = 94 ºC. MS calculated for $C_{29}H_{24}F_{25}NO_5$ = 941.1, MS found = 942.3 $(M+H)^+$. ^{1}H-NMR ($CDCl_3$, 500 MHz) δ/ppm: 1.45 (s, 9H), 2.36-2.50 (m, 2H), 3.68 (dd, 1H, J = 9.4 Hz, J = 3.2 Hz), 3.88 (dd, 1H, J = 9.4 Hz, J = 3.2 Hz), 4.36-4.50 (m, 4H), 4.53 (d, 1H, J = 12.1 Hz), 5.38 (d, 8.9 Hz), 7.21-7.40 (m, 5H). ^{13}C NMR ($CDCl_3$, 125 MHz) δ 170.53, 155.64, 137.53, 128.57, 128.06, 127.82, 80.28, 73.47, 69.92, 57.37, 54.15, 30.61 (t, J = 21.9 Hz), 28.42. IR (ATR): 3421, 1741, 1717, 1495, 1458, 1369, 1340, 1203, 1152, 1125, 1087, 1067, 1029, 1010, 819, 776, 737, 730 cm^{-1}.

4.2.3.14. Synthesis of (S)-3-(benzyloxy)-1-((1H,1H,2H,2H-perfluorotetradecyl)oxy)-1-oxopropan-2-aminium chloride (CF14 b)

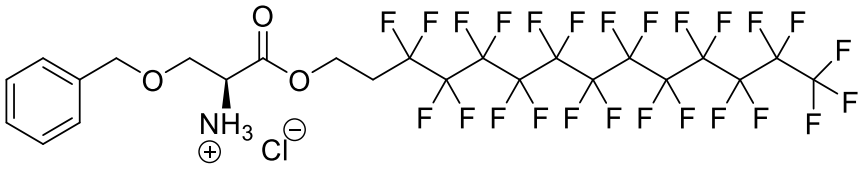

Figure 26 Structure of (S)-3-(benzyloxy)-1-((1H,1H,2H,2H-perfluorotetradecyl)oxy)-1-oxopropan-2-aminium chloride

The compound was synthesized according to the general procedure described at 4.2.2.2. 165 mg of 1H,1H,2H,2H-perfluorotetradecyl *O*-benzyl-*N*-(*tert*-butoxycarbonyl)-L-serinate (0.175 mmol, 1 eq.), 5 ml of 4N HCl in dioxane (25 mmol, 143 eq.), Reaction time was 2 hours. The mobile phase for TLC control was a mixture of *n*-hexane/EtOAc (3/1). 154 mg of the desired product were isolated (yield = 97%) as yellowish crystals, mp = 116-117 ºC. MS calculated for $C_{24}H_{17}F_{25}NO_3^+$ = 842.1, MS found = 842.3. Due to low solubility in common solvents this compound was used in next reaction step with only MS characterization. IR (ATR): 3794, 2920, 1741, 1471, 1355, 1205, 1150, 1074, 836, 747, 700 cm^{-1}.

4.2.3.15. Synthesis of 1H,1H,2H,2H-perfluorotetradecyl *O*-benzyl-*N*-tetracosanoyl-L-serinate (CF14 c)

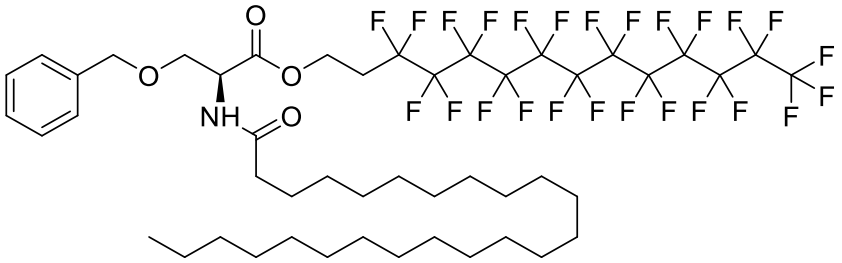

Figure 27 Structure of 1H,1H,2H,2H-perfluorotetradecyl O-benzyl-N-tetracosanoyl-L-serinate

The compound was synthesized according to the general procedure for amidation described at 4.2.2.3. 35 mg of (S)-3-(benzyloxy)-1-(1H,1H,2H,2H-perfluorotetradecyloxy)-1-oxopropan-2-aminium chloride (0.04 mmol, 1 eq.), 15 mg of lignoceric acid (0.04 mmol, 1 eq.), 7 µl of EDC (0.04 mmol, 1 eq.), 6 mg of DMAP (0.04 mmol, 1.1 eq.). Mobile phase for column chromatography was a mixture of *n*-hexane/$CHCl_3$/EtOAc (3/3/0.7). R_f = 0.75 in *n*-hexane/$CHCl_3$/EtOAc (3/3/0.7). 31 mg of the desired product were isolated (yield = 65%) as white crystals, mp = 89 ºC. MS calculated for $C_{48}H_{62}F_{25}NO_4$ = 1191.4 , MS found = 1192.6 $(M+H)^+$. ^{1}H-NMR ($CDCl_3$, 500 MHz) δ/ppm: 0.88 (t, 3H, J = 6.8 Hz), 1.10-1.42 (m, 42H), 2.22 (t, 2H, J = 7.6 Hz), 2.32-2.55 (m, 2H), 3.67 (dd, 1H, J = 9.5 Hz, J = 3.1 Hz), 3.90 (dd, 1H, J = 9.5 Hz, J = 3.1 Hz), 4.34-4.60 (m, 4H), 4.78 (dt, 1H, J = 8.4 Hz, J = 3.1 Hz), 6.23 (d, 1H, 8.4 Hz), 7.17-7.41 (m, 5H).. ^{13}C NMR ($CDCl_3$, 125 MHz) δ 173.19, 170.20, 137.48, 128.61, 128.15, 127.88, 73.50, 69.74, 57.46, 52.57, 36.66, 32.08, 30.59 (t, J = 21.6 Hz), 29.86, 29.82, 29.79, 29.65, 29.51, 29.40, 25.69, 22.84, 14.25. IR (ATR): 2919, 2850, 1750, 1644, 1539, 1473, 1356, 1203, 1151, 1070, 814, 734, 720 cm^{-1}.

4.2.3.16. Synthesis of 1H,1H,2H,2H-perfluorotetradecyl tetracosanoyl-L-serinate (CF14 d)

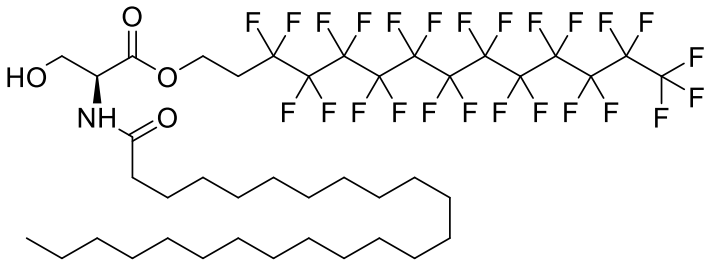

Figure 28 Structure of 1H,1H,2H,2H-perfluorotetradecyl tetracosanoyl-L-serinate

The compound was synthesized according to the general procedure for Bn deprotection described at 4.2.2.4. 85 mg of 1H,1H,2H,2H-perfluorodecyl *O*-benzyl-*N*-tetracosanoyl-L-serinate (0.07 mmol, 1 eq.) was dissolved in a mixture of MeOH/$CHCl_3$

(1/1.5), 80 mg of Pd/C (0.75 mmol, 11 eq.) was added. Reaction time was 24 hours. Mobile phase for TLC control was $CHCl_3$/MeOH (10/1). R_f = 0.50 in $CHCl_3$/MeOH (10/1). 66 mg of the desired product were isolated (yield = 84%) as white crystals, mp = 127 ºC. MS calculated for $C_{41}H_{56}F_{25}NO_4$ = 1101.4, MS found = 1102.6 $(M+H)^+$. ^{1}H-NMR ($CDCl_3$, 500 MHz) δ/ppm: 0.70-0.85 (m, 3H), 1.19 (s, 40H), 1.37-1.49 (m, 2H), 1.87-2.02 (m, 2H), 2.17-2.31 (m, 2H), 3.55-3.72 (m, 5H), 5.28 (s, 1H). Due to low solubility of the compound, signals with expected ppm were found, but the integration and coupling constants could not be evaluated precisely. Also, the carbon NMR could not be measured. However, the MS confirmed the mass of the final compound. IR (ATR): 3534, 2917, 2850, 1730, 1653, 1519, 1473, 1356, 1309, 1212, 1149, 1131, 1110, 1068, 1012, 809, 757, 717 cm^{-1}.

4.3. Permeation experiments

Synthesis was followed by *ex-vivo* permeation experiments. Compounds synthesized above were used for permeation experiments (C10 d, CF10 d, C14 d, CF14 d). Experiments were performed using Franz diffusion cells while human skin was used as a permeation membrane.

4.3.1. Skin and preparation of native and experimentally damaged SC

Human skin was obtained from patients who underwent an abdominal plastic surgery at Sanatorium Sanus, První privátní chirurgické centrum spol. s.r.o in Hradec Králové. The skin was used with approval of the Ethics committee of the Sanus Surgical Centre, according to the principles of the Declaration of Helsinki. Informed consent has been obtained from each individual. Subcutaneous fat was carefully removed with a scalpel after transportation and remaining skin fragments were thoroughly washed, dried, and stored at -20 ˚C. Before the experiment, skin was let to unfreeze at room temperature and checked for any potential damage. Skin pieces were later dermatomed to obtain the final thickness of 500 µm and the dermatomed strips were left to incubate in PBS of pH = 7.4 with addition of 0.5% trypsin in PBS overnight at 32 ˚C. Separated SC was rinsed and placed in water.

Six SC samples were left untreated. The rest of SC samples were damaged by applying a mixture of *n*-hexane:EtOH in different ratios for different time periods. For the first permeation experiment, the damage induced by treating the SC with a mixture of *n*-hexane:EtOH in a ratio of 2:1 for two hours and subsequently with the same mixture of solvents in a ratio of 1:1 for another two hours. For the second permeation experiment, only a milder damage induced by treating the SC with a mixture of *n*-hexane:EtOH in a ratio of 1:1 for five minutes.

4.3.2. Franz diffusion cells

Custom-made Franz diffusion cells were used (Figure 29), which consist of upper donor part and lower acceptor part. Figure 29 is only for illustration, as it contains full thickness skin. For this experiment only SC was used. SC samples were placed on a filter membrane with 0.015 µm pores, enclosed between two Teflon holders, sealed with silicone grease and mounted in the cells by rubber bands. The acceptor part of each cell was filled with PBS (pH = 7.4 with 0.005 g/l gentamycin) while a magnetic stirrer was also placed in the acceptor part. Cells were then left for equilibration overnight at 32 ˚C.

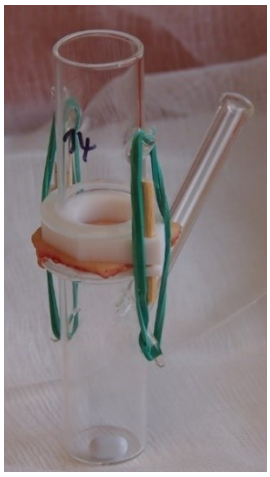

Figure 29 Franz diffusion cell

4.3.3. Measurements, sample preparation and application

Skin damage was controlled by TEWL and EI measurements before and after application. TEWL was measured when the upper part of the Franz cell was removed with an instrument that uses the condenser-chamber measurement method. TEWL measurements are defined by a flux of water diffusing through the membrane. EI was measured after applying 500 µl of PBS in the acceptor phase and subsequently immersing one electrode in the acceptor part and the other electrode in the donor part of the cell. The units of EI measurements were kΩ x cm^2. Samples of the final synthesized compounds were applied in a form of 0.1% suspension in 60% PG:EtOH (7:3) and were sonicated for two hours prior to application. 100 µl of each sample were applied in cells as described in table 3. Cells were left to equilibrate for 12 hours. Applied mixture was then carefully washed away with 500 µl of 60% PG:EtOH (7:3) and 500 µl of Millipore water. After 2 hours TEWL and EI were measured once again. Following the measurement cells were left for equilibration overnight.

Table 3 Application of samples

Properties of SC	Application (100 µl)	Replicates
Non-damaged	No application	6
Damaged	No application	4
Damaged	60% PG:EtOH (7:3)	6
Damaged	C10 d (0.1%) in 60% PG:EtOH (7:3)	6
Damaged	CF10 d (0.1%) in 60% PG:EtOH (7:3)	6
Damaged	C14 d (0.1%) in 60% PG:EtOH (7:3)	6
Damaged	CF14 d (0.1%) in 60% PG:EtOH (7:3)	6

4.3.4. Application of permeant, sampling, and HPLC evaluation

Theophylline was used as a model permeant for this study, and it was applied as a 5% suspension in 60% PG. 100 µl of the prepared suspension were applied in each donor chamber. Samples of 300 µl were taken from lower acceptor part every 2 hours, for a total period of 10 hours with simultaneous refilling of acceptor volume with 300 µl of PBS. Samples were then evaluated by HPLC. The HPLC mobile phase used for the determination of theophylline concentration was a mixture of MeOH:0.1 M NaH_2PO_4 4:6 (v/v) at a flow rate of 1.2 ml/min. Each injection volume was 20 µl. Detection of theophylline was at 272 nm, and its retention time was 3.2 ± 0.1 min. This quantification method has been previously validated.(63)

5. Results and Discussion

Previous results of our research group have proven that tetradecyl tetracosanoyl-L-serinate (Figure 30) has a barrier repairing ability.(59, 62) It consists of an L-serine polar head, one 14 carbon aliphatic chain attached to L-serine by an ester bond and an amide-bonded lignoceric acid (24 carbon aliphatic chain). This structure mimics Cer NS which is naturally found in SC. The only difference is the ester bond replacing an allylic hydroxyl (Figure 30).(59)

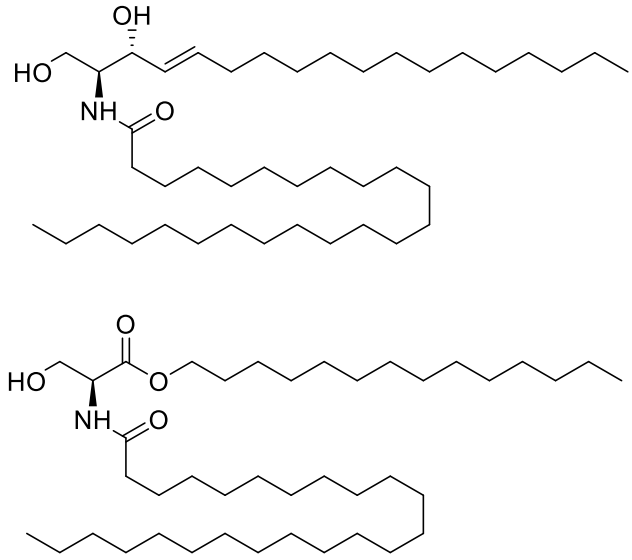

Figure 30 Structure of Cer NS (above) and tetradecyl tetracosanoyl-L-serinate (C14 d) (below)

In a different study of our research group, different derivatives of *N,N*-dimethylamino acid esters (Figure 31) were examined for their permeation enhancing ability.(65)

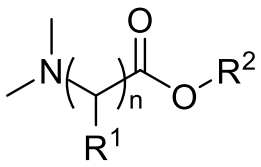

Figure 31 General structure of synthesized N,N-dimethylamino acid esters

One of these derivatives was polyfluorinated. The experimental data showed that polyfluorination has led to complete abolishment of permeation enhancing ability. It was believed, that the abolishment was a result of increase in hydrophobicity and amplified steric repulsions due to polyfluorination, which led to increased rigidity and ordering of skin barrier lipids.(65) This fact led us to examine polyfluorination as an approach to increase

the skin repairing potential of molecules proved to recover perturbed human skin barrier like tetradecyl tetracosanoyl-L-serinate (Figure 30).

5.1. Synthesis

One of the aims of this work was to find a convenient synthesis of polyfluorinated pCer in a sufficient amount for skin permeation experiments. A four-step synthesis scheme was designed using *O*-benzyl-*N*-(*tert*-butyloxycarbonyl)-L-serine as a starting material. The benzyl protection of the L-serine side chain hydroxyl group and the *tert*-butyloxycarbonyl protection of the L-serine amine are offering the ease of ester synthesis at the free L-serine carboxylic group and the subsequent selective deprotection under different experimental conditions.

To examine the effect of the side chain size, alcohols of different chain length (10 and 14 carbons) were used for the ester synthesis reaction. Previous synthetic approaches of our research group (unpublished data) have shown that alcohols with total fluorination of their carbon chain have a very bad solubility in common solvents and the reaction yields are low. Thus, in the present study, only partially fluorinated commercially available alcohols were used, i.e., 1H,1H,2H,2H-perfluorodecanol and 1H,1H,2H,2H-perfluorotetradecanol, to maintain some of the hydrocarbon properties, and thus facilitate solubility improvement. EDC was used as an activating agent and DMAP was used as a base.

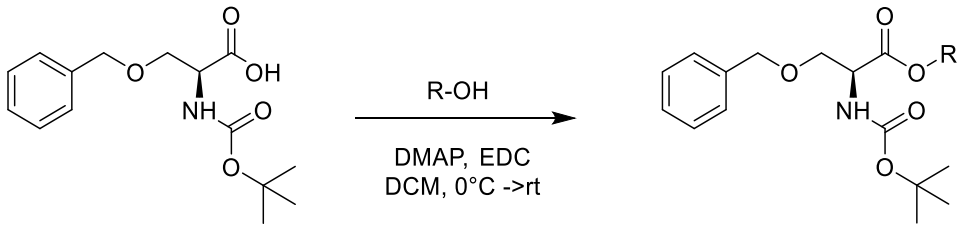

Figure 32 General scheme for ester synthesis reaction

The ester synthesis was expected to be the most problematic step, according to the previous research mentioned earlier. Although yields of fluorinated compounds were lower than of their non-fluorinated analogues, we managed to obtain sufficient amount of product for next reaction steps.

Table 4 Yields for ester synthesis reaction

Compound	R	Yield
C10 a	$CH_3(CH_2)_9$-	52%
CF10 a	$CF_3(CF_2)_7(CH_2)_2$-	21%
C14 a	$CH_3(CH_2)_{13}$-	47%
CF14 a	$CF_3(CF_2)_{11}(CH_2)_2$-	39%

For the deprotection of Boc group, a 4N HCl solution in dioxane was used forming a hydrochloric salt.

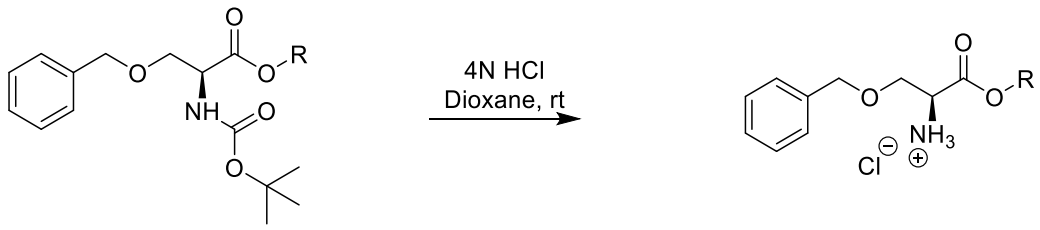

Figure 33 General scheme for Boc deprotection

Table 5 Yields for Boc deprotection

Compound	R	Yield
C10 b	$CH_3(CH_2)_9$-	96%
CF10 b	$CF_3(CF_2)_7(CH_2)_2$-	89%
C14 b	$CH_3(CH_2)_{13}$-	70%
CF14 b	$CF_3(CF_2)_{11}(CH_2)_2$-	96%

The third step was the amidation of the amine end with lignoceric acid, which is a long chain aliphatic acid with 24 hydrocarbon chain. Similar conditions like during the ester synthesis were used.

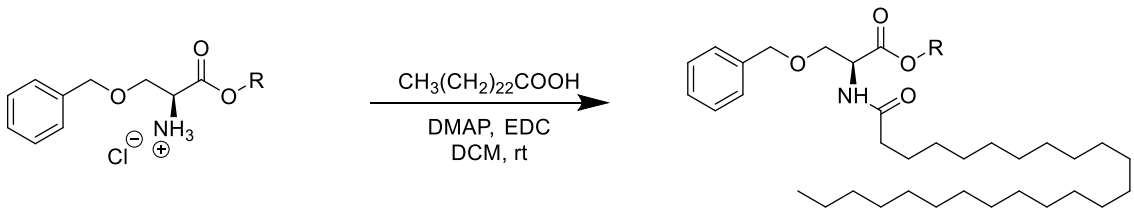

Figure 34 General scheme for amidation

Table 6 Yields for amidation

Compound	R	Yield
C10 c	$CH_3(CH_2)_9$-	40%
CF10 c	$CF_3(CF_2)_7(CH_2)_2$-	72%
C14 c	$CH_3(CH_2)_{13}$-	47%
CF14 c	$CF_3(CF_2)_{11}(CH_2)_2$-	46%

The target compounds were isolated after Bn deprotection (hydrogenation) using hydrogen atmosphere in the presence of palladium on activated carbon as a catalyst.

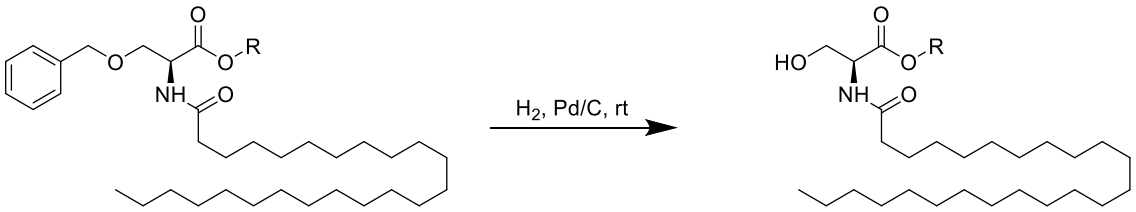

Figure 35 General scheme for Bn deprotection

For the two non-fluorinated compounds, EtOAc was used as a solvent and the reaction proceeded without further complications. On the other hand, the fluorinated compounds had very bad solubility in EtOAc and different solvents were used during this step. More specifically, for these compounds a mixture of MeOH and $CHCl_3$ was used. The fluorinated compound with 10 carbon fluorinated sidechain was sufficiently dissolved in a mixture of MeOH:$CHCl_3$ with a ratio of 7:3. For the compound with 14 carbon fluorinated sidechain, the polarity of the mixture had to be further reduced so the solvent mixture that dissolved the starting material was MeOH:$CHCl_3$ at a ratio of 1:1.5.

Table 7 Yields for Bn deprotection

Compound	R	Yield
C10 d	$CH_3(CH_2)_9$-	98%
CF10 d	$CF_3(CF_2)_7(CH_2)_2$-	99%
C14 d	$CH_3(CH_2)_{13}$-	85%
CF14 d	$CF_3(CF_2)_{11}(CH_2)_2$-	84%

The synthesis resulted in formation of 4 compounds, two non-fluorinated pCer and their fluorinated analogues (Figure 36).

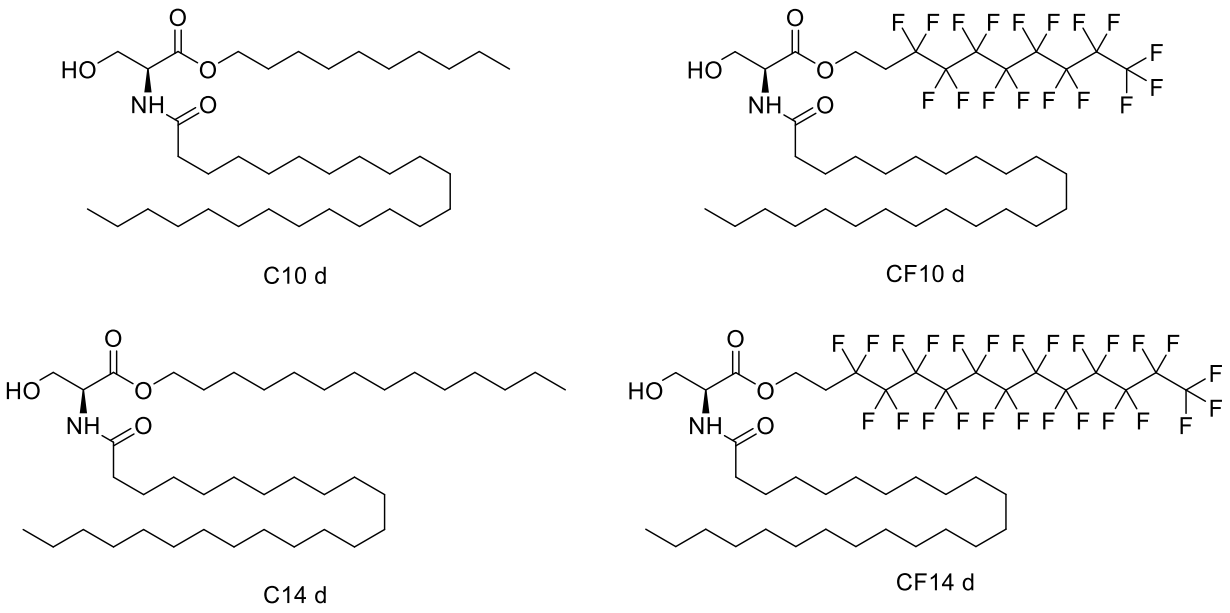

Figure 36 Summary of synthesized final compounds

5.2. Skin permeation experiments

The final synthesized compounds (Figure 36) were used for *ex vivo* skin permeation experiments on human SC as described in chapter 4.3. In the skin permeation experiments undamaged SC was used as a control. C14 d as a known skin repairing agent was used to further compare the impact of fluorination to skin repairing ability of applied compounds. Two permeation experiments were performed during this study and will be separately commented in the next subchapters.

5.2.1. The first permeation experiment

During the first permeation experiment, the isolated SC was damaged by a mixture of *n*-hexane/EtOH in a ratio of 2:1 for two hours and subsequently with the same mixture of solvents in a ratio of 1:1 for another two hours. The rest of the experiment conditions are described in chapter 4.3.

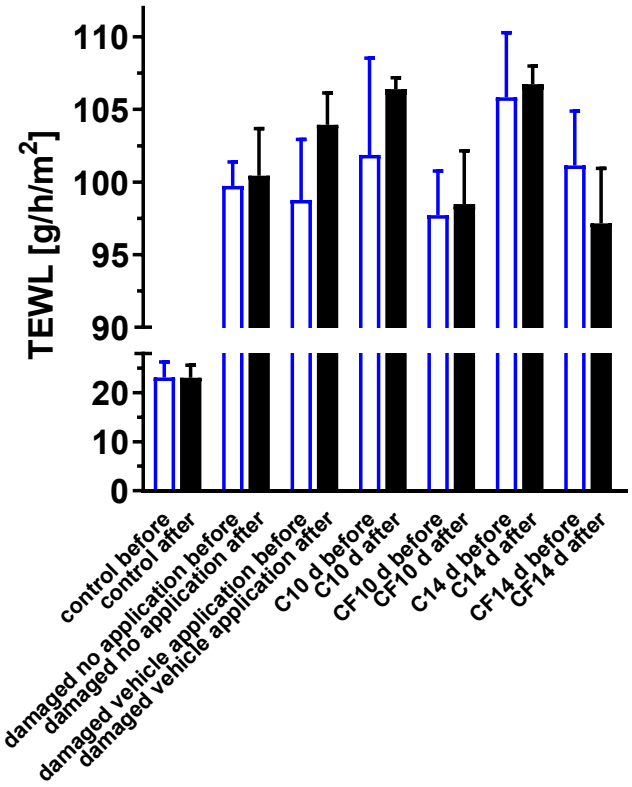

Figure 37 TEWL measurement of the first permeation experiment

TEWL measurements before and after application of compounds are shown in the graph above (Figure 37). The TEWL values for undamaged cells were 23.13 ± 3.15 g/h/m^2. The TEWL results for damaged cells were in a range from 97.15 g/h/m^2 to 106.7 g/h/m^2.

From the TEWL results, it is visible, that the induced damaging to the SC was uncontrollable and even before the compound application the level of damaging was not uniform. In addition, after the compound application, the skin barrier properties did not seem to induce some barrier repairing for the majority of the treated cells. The only visible decrease was observed in cells where CF14 d was applied, where TEWL values dropped from 101.1 ± 3.75 g/h/m^2 to 97.15 ± 3.78 g/h/m^2, however this decrease was not statistically significant.

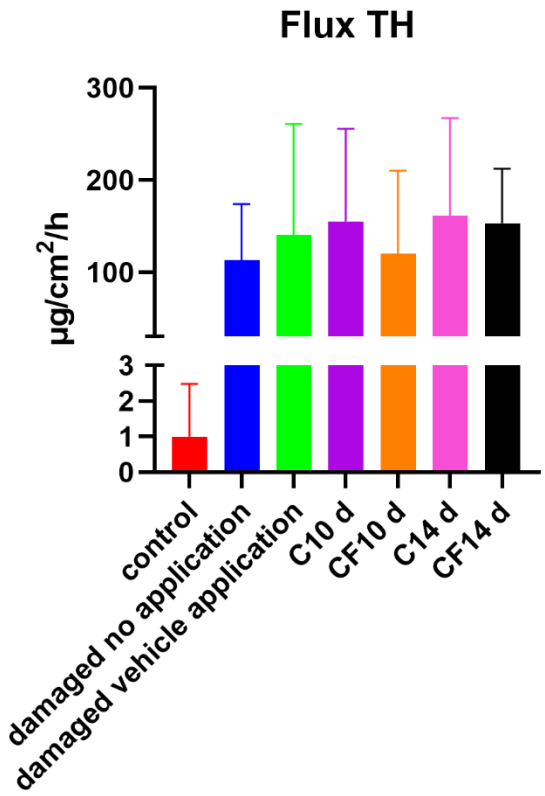

Figure 38 Theophylline permeation profile of the first permeation experiment

Flux of theophylline permeation for the undamaged control cells was 0.99 ± 0.66 ug/cm^2/h. Flux of theophylline for cells with application of C10 d, CF10 d, C14 d and CF14 d was 155.30 ± 41.02 ug/cm^2/h, 120.10 ± 36.81 ug/cm^2/h, 161.30 ± 43.16 ug/cm^2/h and 153.10 ± 24.17 ug/cm^2/h respectively. For the cells where C14 d was applied (which has already proven to have skin repairing abilities) there was no improvement in theophylline permeation profile compared to the controls, actually the flux for these cells was the highest amongst all damaged cells (Figure 38).

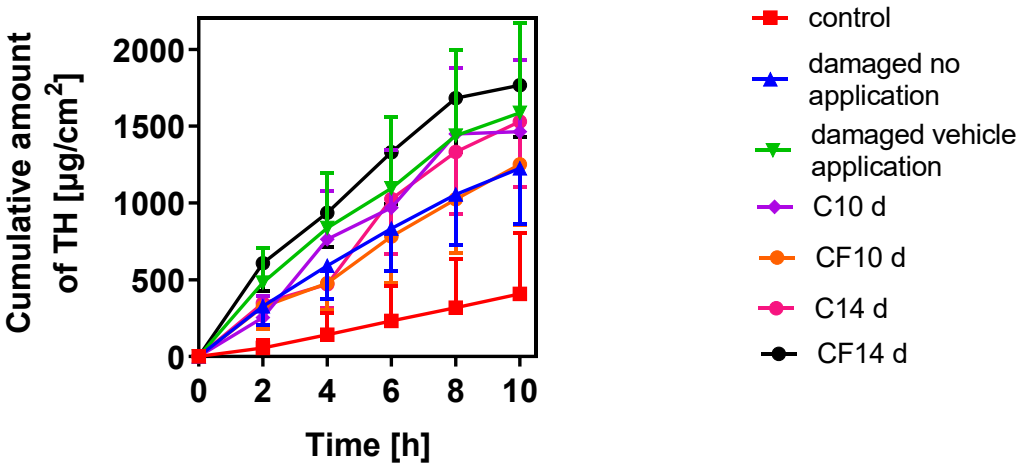

Figure 39 Cumulative theophylline permeation of the first permeation experiment

Value of cumulative theophylline permeation after 10 hours for the undamaged control cells was 407 µg/cm^2. Values of cumulative theophylline permeation after 10 hours for cells with application of C10 d, CF10 d, C14 d and CF14 d was 1465 µg/cm^2, 1252 µg/cm^2, 1529 µg/cm^2 and 1766 µg/cm^2 respectively (Figure 39).

Results from the theophylline permeation (Figures 38 and 39) did not show any significant improvement of skin barrier properties compared to the undamaged SC controls. This further supports the idea that the induced damaging was too severe, since even C14 d did not show improved permeation profile as was expected. The explanation of these results could be, that the compounds were not able to reverse such a harsh damaging of the SC.

5.2.2. The second permeation experiment (with milder SC damage)

The protocol followed during the second permeation experiment was similar to the first with slight modification on the SC treatment time with the organic solvents as described in chapter 4.3. In more detail, the SC was treated with a 1:1 mixture of *n*-hexane/EtOH for five minutes to decrease the level of damaging.

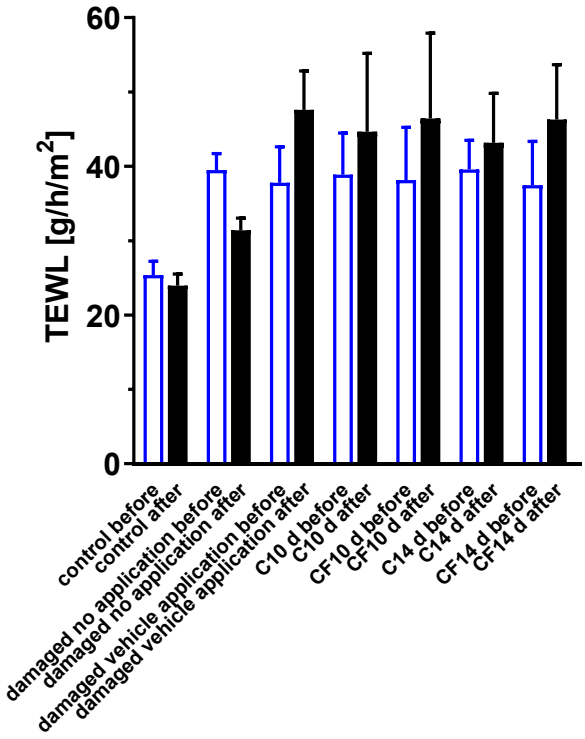

Figure 40 TEWL measurement of the second permeation experiment

TEWL value for undamaged cells was 25.35 ± 1.86 g/h/m^2. TEWL range of the cells that have undergone damaging was from 37.46 g/h/m^2 to 39.56 g/h/m^2 before application of compounds (Figure 40). In comparison to the TEWL measurements (Figure 37) from the first permeation experiment mentioned in previous chapter (5.2.1), it is apparent that the induced damaging to the SC was performed in a much more controlled way and resulted in more favorable TEWL profile for majority of measured cells.

An increase in TEWL from 37.79 ± 4.83 g/h/m^2 to 47.60 ± 5.22 g/h/m^2 was observed for the cells where only the vehicle (60% PG and EtOH in a ratio of 7:3) was applied, which may suggest that the selected vehicle is further damaging the SC. Though, the noticed TEWL difference was not statistically significant. A similar trend was observed for all the cells treated with the synthesized compounds, where the TEWL values were in range from 43.16 g/h/m^2 to 46.43 g/h/m^2, again without statistically significant differences. Notably, a slight TEWL decrease was observed for the cells which left untreated (again with no statistical significance). In this case the TEWL values have dropped from 39.49 ± 2.21 g/h/m^2 to 31.31 ± 1.65 g/h/m^2. We would expect a decrease in TEWL levels at least for the cells where C14

d was applied but this was not the case. Thus, the TEWL data may suggest that the vehicle choice was not ideal and further research is needed on this direction.

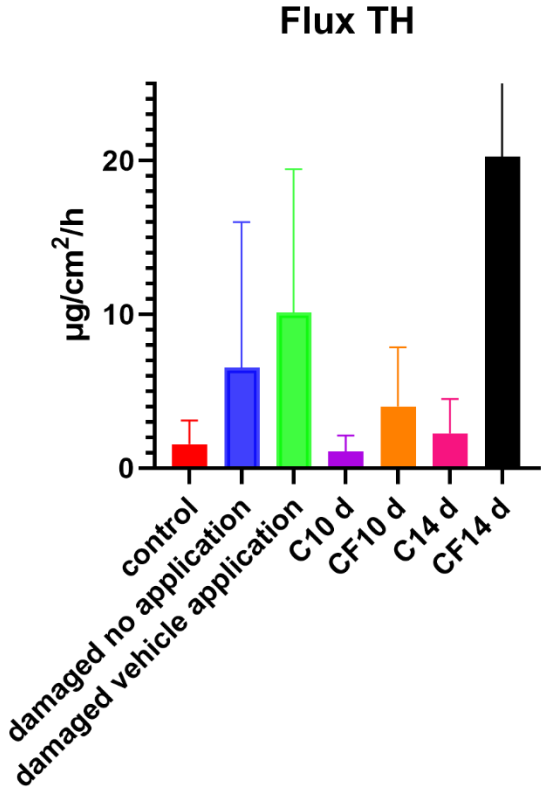

Figure 41 Flux theophylline permeation of the second permeation experiment

Compared to previous permeation experiment (5.2.1), amount of theophylline that permeated through the SC has decreased significantly. Cells with undamaged SC maintained similar values of 1.56 ± 0.63 ug/cm^2/h. Cells with damaged SC treated with the compounds C10 d, CF10 d, C14 d and CF14 d had theophylline flux values of 1.08 ± 0.47 ug/cm^2/h, 4.01 ± 1.58 ug/cm^2/h, 2.27 ± 0.91 ug/cm^2/h and 20.27 ± 10.72 ug/cm^2/h respectively. For the cells with damaged SC and no application or only vehicle application values of the flux are 6.52 ± 4.74 ug/cm^2/h and 10.12 ± 9.32 ug/cm^2/h respectively. Comparison of these two values could represent the assumed damaging of the SC by only the vehicle, since the value of cells after the vehicle application is higher than without the application (Figure 41).

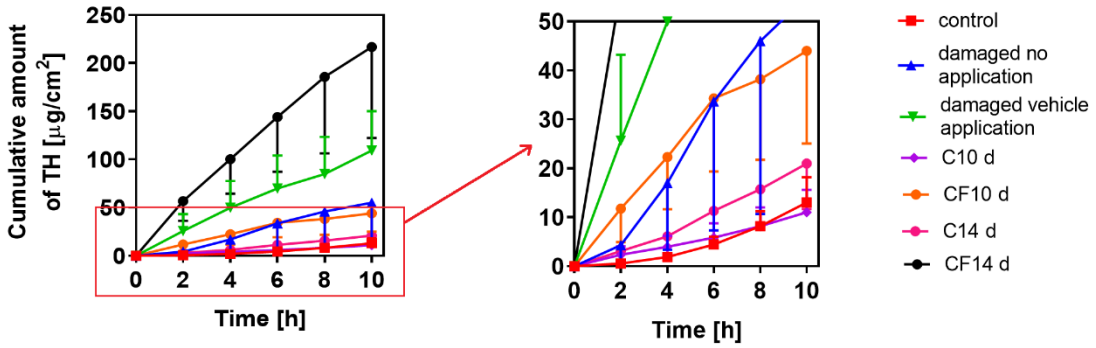

Figure 42 Theophylline permeation profile of the second permeation experiment

Value of cumulative theophylline permeation after 10 hours for the undamaged control cells was 11.04 ± 2.07 µg/cm^2. Values of cumulative theophylline permeation after 10 hours for cells with application of C10 d, CF10 d, C14 d and CF14 d was 11.00 ± 1.63 µg/cm^2, 43.98 ± 6.90 µg/cm^2, 20.99 ± 3.25 µg/cm^2 and 216.70 ± 33.17 µg/cm^2 respectively. Values of cumulative theophylline permeation after 10 hours for cells with no application and only vehicle application were 55.02 ± 22.48 µg/cm^2 and 109.3 ± 16.30 µg/cm^2 respectively (Figure 42).

The amount of theophylline that permeated to the acceptor phase has dropped significantly for the cells where C14 d was applied in comparison to damaged cells with no vehicle application or with vehicle application. This outcome is confirming the expected barrier repairing function of this compound which was previously found.(62) Along with C14 d, also C10 d has shown a similar effect. Permeation profile of both compounds could be compared to the profile of the undamaged SC controls. The same behavior was not observed for the fluorinated compounds (CF10 d and CF14 d). In fact, CF14 d has manifested the worst permeation profile of all tested compounds. This could mean that the fluorination does not have any beneficial effect on skin repairing ability of the compounds. However, it is vital to discuss the solubility of the fluorinated compounds. Even though the samples were applied in a form of 0.1% suspension, the non-fluorinated compounds have shown a much better solubility in the vehicle after two-hour sonication. Solubility have worsened with higher extent of fluorination as well as with higher length of the aliphatic chain. Comparable results are found in theophylline permeation, where C10 d has the most promising profile, and it worsens in compounds with longer aliphatic chains and extent of fluorination respectively, with CF14 d having the worst results. This observation could further support the idea that the effect of the fluorinated compounds on the skin barrier was

not representatively demonstrated because of lower solubility in the vehicle compared to non-fluorinated analogues.

In order to examine the effect of polyfluorination of the compounds on skin barrier properties, the future approach is to investigate alternative application conditions. Incorporating the compounds in a cream or liposomes could be a beneficial approach to aid the access of polyfluorinated pCer to the SC while maintaining the properties of their non-fluorinated analogues.

6. Conclusion

The first aim of this work was to find a convenient synthesis of ceramide analogues with partially fluorinated sidechain and their non-fluorinated analogues. This was achieved by a four-step synthesis resulting in a formation of two fluorinated compounds, with 10 and 14 carbon fluorinated aliphatic sidechain, and two analogous non-fluorinated compounds.

The second aim was to evaluate the effect of fluorination on skin repairing ability of the compounds. This was carried out by skin permeation experiments. The preliminary skin permeation experiments have confirmed the previous results of the non-fluorinated compound C14 d and have shown some potential of the non-fluorinated compound C10 d to have similar if not improved skin repairing ability. The polyfluorination did not result in enhanced repairing ability of the compounds. This could mean that the polyfluorination is not beneficial for the skin repairing ability. However, the low solubility of the compounds could lead to insufficient effect on the damaged SC, and thus the demonstration of the effect could be considerably limited.

A future direction is to examine alternative application conditions for the compounds to observe the effect of the compounds' fluorination on skin barrier properties more reliably. One of the approaches would be to incorporate compounds into a cream or liposomes and perform the permeation experiments with this formulation. This could resolve the issue with solubility, and additionally it would potentially remove the further damaging of the SC by the used vehicle.

7. References

1. Kanitakis J. Anatomy, histology and immunohistochemistry of normal human skin. Eur J Dermatol. 2002;12(4):390-399.

2. Číhak R. Anatomie. 3 ed: Grada; 2016. 832 p.

3. Turkington C, Dover JS. Skin Deep: Facts on File; 2007.

4. Yousef H, Alhajj M, Sharma S. Anatomy, Skin (Integument), Epidermis. StatPearls. Treasure Island (FL): StatPearls Publishing; 2022.

5. Khavkin J, Ellis DA. Aging skin: histology, physiology, and pathology. Facial Plast Surg Clin North Am. 2011;19(2):229-234.

6. McLafferty E. The integumentary system: anatomy, physiology and function of skin. Nurs Stand. 2012;27(3):35-42.

7. Freeman SC, Sonthalia S. Histology, Keratohyalin Granules. StatPearls. Treasure Island (FL): StatPearls Publishing Copyright © 2022, StatPearls Publishing LLC.; 2022.

8. Ramadon D, McCrudden MTC, Courtenay AJ, Donnelly RF. Enhancement strategies for transdermal drug delivery systems: current trends and applications. Drug Deliv Transl Res. 2022;12(4):758-791.

9. Sahle FF, Gebre-Mariam T, Dobner B, Wohlrab J, Neubert RH. Skin diseases associated with the depletion of stratum corneum lipids and stratum corneum lipid substitution therapy. Skin Pharmacol Physiol. 2015;28(1):42-55.

10. Michaels AS, Chandrasekaran SKD, Shaw JE. Drug permeation through human skin: Theory and invitro experimental measurement. Aiche Journal. 1975;21:985-996.

11. Proksch E, Brandner JM, Jensen JM. The skin: an indispensable barrier. Exp Dermatol. 2008;17(12):1063-1072.

12. Hatfield RM, Fung LW. Molecular properties of a stratum corneum model lipid system: large unilamellar vesicles. Biophys J. 1995;68(1):196-207.

13. Menon GK, Elias PM. Structural and Lipid Biochemical Correlates of the Epidermal Permeability Barrier. Skin Lipids. 24: Elsevier; 1991. p. 1-26.

14. Del Rosso JQ, Levin J. Clinical relevance of maintaining the structural and functional integrity of the stratum corneum: why is it important to you? Journal of drugs in dermatology: JDD. 2011;10(10 Suppl):s5-s12.

15. Kolter T, Sandhoff K. Sphingolipid metabolism diseases. Biochimica et Biophysica Acta (BBA)-Biomembranes. 2006;1758(12):2057-2079.

16. Meckfessel MH, Brandt S. The structure, function, and importance of ceramides in skin and their use as therapeutic agents in skin-care products. J Am Acad Dermatol. 2014;71(1):177-184.

17. Masukawa Y, Narita H, Shimizu E, Kondo N, Sugai Y, Oba T, et al. Characterization of overall ceramide species in human stratum corneum. J Lipid Res. 2008;49(7):1466-1476.

18. Li Q, Fang H, Dang E, Wang G. The role of ceramides in skin homeostasis and inflammatory skin diseases. J Dermatol Sci. 2020;97(1):2-8.

19. Zwara A, Wertheim-Tysarowska K, Mika A. Alterations of Ultra Long-Chain Fatty Acids in Hereditary Skin Diseases-Review Article. Front Med (Lausanne). 2021;8:730855.

20. Coderch L, López O, de la Maza A, Parra JL. Ceramides and skin function. Am J Clin Dermatol. 2003;4(2):107-129.

21. Smeden JV, Bouwstra JA. Stratum Corneum Lipids: Their Role for the Skin Barrier Function in Healthy Subjects and Atopic Dermatitis Patients. Curr Probl Dermatol. 2016;49:8-26.

22. Janssens M, van Smeden J, Gooris GS, Bras W, Portale G, Caspers PJ, et al. Increase in short-chain ceramides correlates with an altered lipid organization and decreased barrier function in atopic eczema patients. J Lipid Res. 2012;53(12):2755-2766.

23. Choi MJ, Maibach HI. Role of ceramides in barrier function of healthy and diseased skin. Am J Clin Dermatol. 2005;6(4):215-223.

24. Rabionet M, Gorgas K, and Sandhoff R. Ceramide synthesis in the epidermis. Biochimica et Biophysica Acta (BBA) - Molecular and Cell Biology of Lipids. 2014;1841(3):422-434.

25. Han G, Gupta SD, Gable K, Niranjanakumari S, Moitra P, Eichler F, et al. Identification of small subunits of mammalian serine palmitoyltransferase that confer distinct acyl-CoA substrate specificities. Proceedings of the National Academy of Sciences. 2009;106(20):8186-8191.

26. Mizutani Y, Mitsutake S, Tsuji K, Kihara A, Igarashi Y. Ceramide biosynthesis in keratinocyte and its role in skin function. Biochimie. 2009;91(6):784-790.

27. Akio K. Synthesis and degradation pathways, functions, and pathology of ceramides and epidermal acylceramides. Progress in Lipid Research. 2016;63:50-69.

28. Mizutani Y, Kihara A, Igarashi Y. Mammalian Lass6 and its related family members regulate synthesis of specific ceramides. Biochem J. 2005;390(Pt 1):263-271.

29. Kitatani K, Idkowiak-Baldys J, Hannun YA. The sphingolipid salvage pathway in ceramide metabolism and signaling. Cell Signal. 2008;20(6):1010-1018.

30. Chatelut M, Leruth M, Harzer K, Dagan A, Marchesini S, Gatt S, et al. Natural ceramide is unable to escape the lysosome, in contrast to a fluorescent analogue. FEBS Lett. 1998;426(1):102-106.

31. Riboni L, Bassi R, Caminiti A, Prinetti A, Viani P, Tettamanti G. Metabolic fate of exogenous sphingosine in neuroblastoma neuro2A cells. Dose-dependence and biological effects. Ann N Y Acad Sci. 1998;845:46-56.

32. Sassa T, Kihara A. Metabolism of very long-chain Fatty acids: genes and pathophysiology. Biomol Ther (Seoul). 2014;22(2):83-92.

33. Hama H. Fatty acid 2-Hydroxylation in mammalian sphingolipid biology. Biochim Biophys Acta. 2010;1801(4):405-414.

34. Ohno Y, Nakamichi S, Ohkuni A, Kamiyama N, Naoe A, Tsujimura H, et al. Essential role of the cytochrome P450 CYP4F22 in the production of acylceramide, the key lipid for skin permeability barrier formation. Proc Natl Acad Sci U S A. 2015;112(25):7707-7712.

35. Takagi Y, Nakagawa H, Matsuo N, Nomura T, Takizawa M, Imokawa G. Biosynthesis of acylceramide in murine epidermis: characterization by inhibition of glucosylation and deglucosylation, and by substrate specificity. J Invest Dermatol. 2004;122(3):722-729.

36. Pichery M, Huchenq A, Sandhoff R, Severino-Freire M, Zaafouri S, Opálka L, et al. PNPLA1 defects in patients with autosomal recessive congenital ichthyosis and KO mice sustain PNPLA1 irreplaceable function in epidermal omega-O-acylceramide synthesis and skin permeability barrier. Hum Mol Genet. 2017;26(10):1787-1800.

37. Berke R, Singh A, Guralnick M. Atopic dermatitis: an overview. Am Fam Physician. 2012;86(1):35-42.

38. Nutten S. Atopic dermatitis: global epidemiology and risk factors. Ann Nutr Metab. 2015;66 Suppl 1:8-16.

39. Tollefson MM, Bruckner AL, et al. Atopic Dermatitis: Skin-Directed Management. Pediatrics. 2014;134(6):e1735-e1744.

40. Di Nardo A, Wertz P, Giannetti A, Seidenari S. Ceramide and cholesterol composition of the skin of patients with atopic dermatitis. Acta Derm Venereol. 1998;78(1):27-30.

41. Matsumoto M, Umemoto N, Sugiura H, Uehara M. Difference in ceramide composition between "dry" and "normal" skin in patients with atopic dermatitis. Acta Derm Venereol. 1999;79(3):246-247.

42. Park YH, Jang WH, Seo JA, Park M, Lee TR, Kim DK, et al. Decrease of ceramides with very long-chain fatty acids and downregulation of elongases in a murine atopic dermatitis model. J Invest Dermatol. 2012;132:476-479.

43. Jennemann R, Rabionet M, Gorgas K, Epstein S, Dalpke A, Rothermel U, et al. Loss of ceramide synthase 3 causes lethal skin barrier disruption. Human Molecular Genetics. 2011;21(3):586-608.

44. Oizumi A, Nakayama H, Okino N, Iwahara C, Kina K, Matsumoto R, et al. Pseudomonas-derived ceramidase induces production of inflammatory mediators from human keratinocytes *via* sphingosine-1-phosphate. PLoS One. 2014;9(2):e89402.

45. Severity scoring of atopic dermatitis: the SCORAD index. Consensus Report of the European Task Force on Atopic Dermatitis. Dermatology. 1993;186(1):23-31.

46. Chamlin SL, Kao J, Frieden IJ, Sheu MY, Fowler AJ, Fluhr JW, et al. Ceramide-dominant barrier repair lipids alleviate childhood atopic dermatitis: changes in barrier function provide a sensitive indicator of disease activity. J Am Acad Dermatol. 2002;47(2):198-208.

47. Silverberg JI. Atopic dermatitis: an evidence-based treatment update. Am J Clin Dermatol. 2014;15(3):149-164.

48. Boehncke WH, Schön MP. Psoriasis. The Lancet. 2015;386(9997):983-994.

49. Christophers E. Psoriasis--epidemiology and clinical spectrum. Clin Exp Dermatol. 2001;26(4):314-320.

50. Schön MP, Boehncke WH. Psoriasis. N Engl J Med. 2005;352(18):1899-1912.

51. Basavaraj KH, Ashok NM, Rashmi R, Praveen TK. The role of drugs in the induction and/or exacerbation of psoriasis. Int J Dermatol. 2010;49(12):1351-1361.

52. Motta S, Monti M, Sesana S, Caputo R, Carelli S, Ghidoni R. Ceramide composition of the psoriatic scale. Biochimica et Biophysica Acta (BBA) - Molecular Basis of Disease. 1993;1182(2):147-151.

53. Wertz PW, Cho ES, Downing DT. Effect of essential fatty acid deficiency on the epidermal sphingolipids of the rat. Biochim Biophys Acta. 1983;753(3):350-355.

54. Greaves MW, Weinstein GD. Treatment of Psoriasis. New England Journal of Medicine. 1995;332(9):581-589.

55. Hon KL, Leung AK. Use of ceramides and related products for childhood-onset eczema. Recent Pat Inflamm Allergy Drug Discov. 2013;7(1):12-19.

56. Hon KL, Leung AK, Barankin B. Barrier repair therapy in atopic dermatitis: an overview. Am J Clin Dermatol. 2013;14(5):389-399.

57. Proksch E, Jensen JM, Elias PM. Skin lipids and epidermal differentiation in atopic dermatitis. Clin Dermatol. 2003;21(2):134-144.

58. Frankel A, Sohn A, Patel RV, Lebwohl M. Bilateral comparison study of pimecrolimus cream 1% and a ceramide-hyaluronic acid emollient foam in the treatment of patients with atopic dermatitis. J Drugs Dermatol. 2011;10(6):666-672.

59. Vávrová K, Zbytovská J, Palát K, Holas T, Klimentová J, Hrabálek A, et al. Ceramide analogue 14S24 ((S)-2-tetracosanoylamino-3-hydroxypropionic acid tetradecyl ester) is effective in skin barrier repair in vitro. Eur J Pharm Sci. 2004;21(5):581-587.

60. Imokawa G, Yada Y, Higuchi K, Okuda M, Ohashi Y, Kawamata A. Pseudo-acylceramide with linoleic acid produces selective recovery of diminished cutaneous barrier function in essential fatty acid-deficient rats and has an inhibitory effect on epidermal hyperplasia. The Journal of Clinical Investigation. 1994;94(1):89-96.

61. Ishida K, Takahashi A, Bito K, Draelos Z, Genji I. Treatment with Synthetic Pseudoceramide Improves Atopic Skin, Switching the Ceramide Profile to a Healthy Skin

Phenotype. Journal of Investigative Dermatology. 2020;140(9):1762-1770.e8.

62. Vávrová K, Hrabálek A, Mac-Mary S, Humbert P, Muret P. Ceramide analogue 14S24 selectively recovers perturbed human skin barrier. Br J Dermatol. 2007;157(4):704-712.

63. Lv J, Cheng Y. Fluoropolymers in biomedical applications: state-of-the-art and future perspectives. Chem Soc Rev. 2021;50(9):5435-5467.

64. Müller K, Faeh C, Diederich F. Fluorine in pharmaceuticals: looking beyond intuition. Science. 2007;317(5846):1881-1886.

65. Novotný J, Kovaríková P, Novotný M, Janůsová B, Hrabálek A, Vávrová K. Dimethylamino acid esters as biodegradable and reversible transdermal permeation enhancers: effects of linking chain length, chirality and polyfluorination. Pharm Res. 2009;26(4):811-821.

66. McCreery MJ, Skin exposure reduction paste againts chemical warfare agents (SERPACWA), U.S. Patent 5,607,979, 4 March 1997.

67. Braue EH, Jr., Smith KH, Doxzon BF, Lumpkin HL, Clarkson ED. Efficacy studies of Reactive Skin Decontamination Lotion, M291 Skin Decontamination Kit, 0.5% bleach, 1% soapy water, and Skin Exposure Reduction Paste Against Chemical Warfare Agents, part 1: guinea pigs challenged with VX. Cutan Ocul Toxicol. 2011;30(1):15-28.

68. Školová B, Kováčik A, Tesař O, Opálka L, Vávrová K. Phytosphingosine, sphingosine and dihydrosphingosine ceramides in model skin lipid membranes: permeability and biophysics. Biochim Biophys Acta Biomembr. 2017;1859(5):824-834.